Key Points:
- The compensation statistic can determine the handoff between autogenic and allogenic sedimentation even from low-quality data sets
- Topographic relief can be inferred from ancient fluvial and deltaic deposits using the compensation statistic
- The compensation statistic can be successfully applied to natural data from a broad range of extents and resolutions

Correspondence to:
S. M. Trampush,
smt254@psu.edu

Identifying autogenic sedimentation in fluvial-deltaic stratigraphy: Evaluating the effect of outcrop-quality data on the compen sation statistic

S. M. Trampush[1] (iD)**, E. A. Hajek[1]** (iD)**, K. M. Straub[2], and E. P. Chamberlin[1,3]**

[1]Department of Geosciences, Pennsylvania State University, University Park, Pennsylvania, USA, [2]Department of Earth and Environmental Sciences, Tulane University of Louisiana, New Orleans, Louisiana, USA, [3]Now at the Department of Geosciences, Denison University, Granville, Ohio, USA

Abstract Stratigraphy preserves an extensive record of Earth-surface dynamics acting over a range of scales in a variety of environments. To take advantage of this record, we first must distinguish depositional patterns that arise due to intrinsic (i.e., autogenic) landscape dynamics from sedimentation that results from changes in climate, tectonic, or eustatic boundary conditions. The compensation statistic is a quantitative tool that has been used to estimate scales and patterns of autogenic sedimentation in experimental deposits; it has been applied to a few outcrop studies, but its sensitivity to data limitations common in natural deposits remains unconstrained. To explore how the compensation statistic may be applied to outcrop data, we evaluate the sensitivity of the tool to stratigraphic data sets limited in extent and resolution by subsampling an autogenic experimental deposit to create pseudo-outcrop-scale data sets. Results show that for data sets more than 3 times thicker than a characteristic depositional element (e.g., channel or lobe), the compensation statistics that can be used reliably constrain the maximum scale of autogenic sedimentation even for low-resolution data sets. Additionally, we show that autogenic sedimentation patterns may be characterized as persistent, random, or compensational using the compensation statistic when data sets are high resolution. We demonstrate how these measurements can be applied to natural data sets with comparative case studies of two fluvial and two deltaic outcrops. These case studies show how the compensation statistic can provide insight into what controls the maximum scale of autogenic sedimentation in different systems and how landscape dynamics can produce organized sedimentation patterns over long time scales.

1. Introduction

Our ability to use stratigraphy to understand Earth history is limited by how well we can distinguish intrinsic (autogenic) behavior from external (allogenic) environmental forcing in sedimentary deposits. Autogenic processes, such as channel avulsion or delta-lobe switching, have the potential to remove all evidence of low-magnitude or high-frequency climate or tectonic changes from the sedimentary archive, a phenomenon that *Jerolmack and Paola* [2010] call "signal shredding." The maximum scale of autogenic sedimentation in a landscape may set the upper limit of this signal-shredding regime [*Jerolmack and Paola*, 2010; *Wang et al.*, 2011; *Ganti et al.*, 2014; *Li et al.*, 2016]. This means that over small spatial and temporal scales, stratigraphic patterns may reflect dominantly autogenic landscape variations and signals of allogenic processes (such as climate or sea level changes altering the balance of sediment supply and accommodation creation) will dominate sedimentation patterns at larger scales, but what sets the scale between these two behaviors is heavily dependent on the particulars of the system under consideration [*Jerolmack and Paola*, 2010; *Wang et al.*, 2011; *Ganti et al.*, 2014]. Consequently, to know whether a given deposit reflects predominantly landscape dynamics or significant changes in climate, for example, we need tools for identifying the scale (thickness and width) at which this handoff from autogenic to allogenic sedimentation occurs. A key outstanding question is how can autogenic and allogenic scales be identified in natural stratigraphy? In channelized fluvial and deltaic systems, there is evidence that the maximum scale of autogenic sedimentation is the maximum channel depth [*Straub et al.*, 2009; *Wang et al.*, 2011] or greater [*Hajek et al.*, 2010; *Wang et al.*, 2011; *Chamberlin et al.*, 2016]. It is unclear why the autogenic limit in some systems scales with a characteristic channel depth but is significantly greater in others. To answer this question maximum autogenic scale needs to be measured in more deposits from a diverse range of settings, and the uncertainty of these measurements needs to be estimated to facilitate robust comparison.

Physical and numerical experimental studies have established methods to evaluate scales of autogenic organization in fluvial and deltaic systems; a key challenge, however, is applying these approaches and insights to natural systems where data availability is, at best, sparser by several orders of magnitude compared to experimental data sets. The compensation statistic is one tool that has been successfully applied to physical experiments and numerical models in order to evaluate autogenic sedimentation patterns and scales [*Straub et al.*, 2009; *Wang et al.*, 2011; *Straub and Wang*, 2013]. It has also been applied to some ancient natural systems, including fluvial [*Wang et al.*, 2011; *Chamberlin et al.*, 2016], debris flows [*Pederson et al.*, 2015], and deepwater systems [*Straub and Pyles*, 2012]. Despite its promise as a tool, the degree to which sparse sampling affects the accuracy and interpretability of the compensation statistic has not previously been evaluated; consequently, the degree to which the results from one study may be compared to other studies is unknown. Similarly, there remain outstanding questions about the precision with which allogenic scales and autogenic organization can be measured using the compensation statistic.

In order to appropriately use the compensation statistic in natural deposits, it is necessary to determine how the maximum autogenic scale may be determined and the degree to which measures of autogenic organization may be compared among different systems. Here we address these issues by evaluating high-resolution data from a physical experiment and demonstrate how autogenic scale and organization can be measured in outcrop data sets. First, we show how topographic relief in an experimental fluvial-deltaic system is expressed in compensation plots and how we can use these plots to identify scales of autogenic sedimentation. We then explore how subsampling experimental data to typical outcrop resolution affects our ability to measure maximum autogenic scale and autogenic sedimentation patterns. Finally, we apply this insight to a pair of case-study comparisons where we evaluate outcrop data of ancient fluvial and deltaic successions.

2. Background

Compensation describes the tendency of depositional events to preferentially fill topographic lows, smoothing out topographic relief by "compensating" for the localization of sedimentation in discrete landform elements. The term "compensational stacking" has been used to qualitatively describe the large-scale architecture of deep-water, fluvial, and delta deposits [e.g., *Van Wagoner and Mitchum*, 1990; *Olariu and Bhattacharya*, 2006], wherein the sediment-transport network episodically reorganizes along regional topographic lows during channel or lobe avulsions. *Straub et al.* [2009] and others [*Sheets et al.*, 2002; *Lyons*, 2004; *Wang et al.*, 2011; *Straub and Pyles*, 2012] have established a quantitative way of characterizing the tendency for a given depositional system to organize compensationally; we call this metric the *compensation statistic*.

The compensation statistic compares observed sedimentation patterns to what would be expected from uncorrelated random deposition by evaluating the standard deviation of sedimentation across a basin over a range of chronostratigraphic windows (e.g., Figure 1). For experiments, the compensation statistic can be measured with respect to absolute time, since the entire depositional history of an experimental deposit is known. In ancient deposits, where high-resolution age control is often unobtainable, the compensation statistic can be evaluated over a range of characteristic sediment-package thicknesses defined by pseudo-chronostratigraphic surfaces identifiable in outcrop, well, or seismic data (e.g., Figure 1b). These surfaces could include stratal termination (e.g., truncation, downlap, or onlap) surfaces, marker beds, facies boundaries, bed-set boundaries, or other relative timelines that can be mapped within a given deposit.

Over a range of chronostratigraphic intervals, the compensation statistic (*CV*) is the standard deviation of the thickness of a given sediment package across a basin of width *L* relative to the expected average sediment-package thickness across the basin ($\Delta\bar{\eta}_{A,B}$) [*Wang et al.*, 2011; *Straub and Pyles*, 2012].

$$CV = \left\{ \int_L \left[\frac{\Delta\eta_{A,B}(x)}{\Delta\bar{\eta}_{A,B}} \right]^2 dL \right\}^{1/2} \tag{1}$$

where $\Delta\bar{\eta}_{A,B} = \frac{T}{n} i$.

In the case of chronostratigraphic packages lacking absolute time constraints, the expected average sediment-package thickness ($\Delta\bar{\eta}_{A,B}$) is derived from the average thickness of the entire deposit (*T*), the total number of chronostratigraphic surfaces (*n*), and the number of chronostratigraphic surfaces that separate surface *A* from surface *B* (*i*). For all chronostratigraphic pairs with similar measured mean thickness ($\Delta\bar{\eta}_m$),
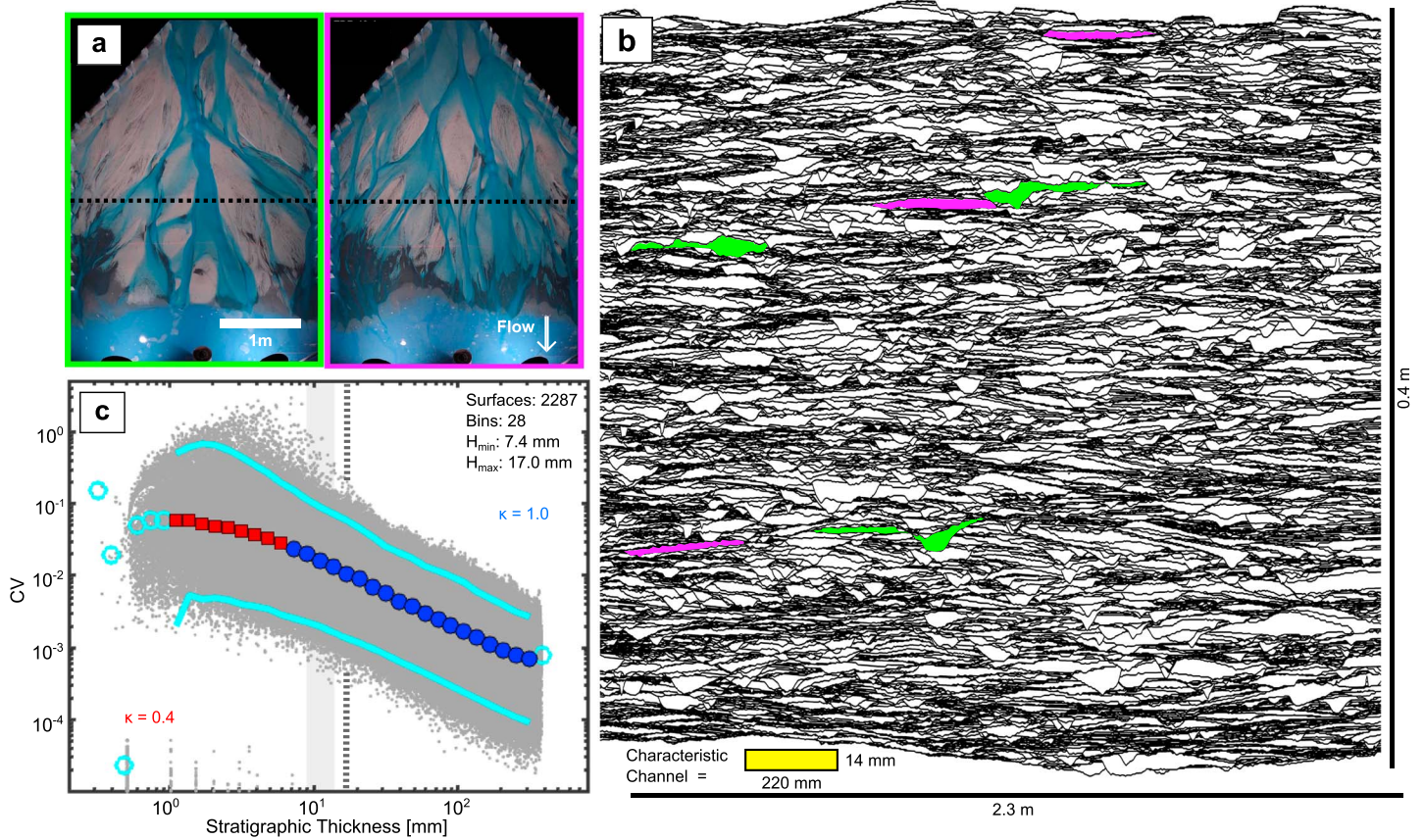
Figure 1. TDB-10-01 is a physical experimental delta that was constructed by self-formed channels under constant sediment- and water-supply conditions and constant base-level rise [*Wang et al.*, 2011; *Straub and Esposito*, 2013; *Straub and Wang*, 2013]. (a) Overhead photos of the experiment show channels in blue, and the intensity of blue dye approximates local flow depth. The active channel network on the delta is sometimes highly localized (e.g., green) or broadly distributed into sheet flows (e.g., magenta). Data used in this study come from laser-topography scans collected 2.13 m downstream from the sediment-water infeed (dashed black line). (b) Stratigraphic cross section of the TDB-10-01 experiment generated using topography scans collected every 2 min throughout the duration of the run. The topographic scans were clipped so that only chronostratigraphic surfaces that were not later eroded remain in the data set. These preserved chronostratigraphic surfaces are used to calculate the compensation statistic in Figure 1c. The yellow rectangle shows a characteristic channel dimension corresponding to the 90th percentile depth and a typical width of a single channel. The colored sand bodies represent high *CV* surface pairs that results from highly channelized deposits (green) and low *CV* surface pairs that result from sheet-flow deposits (magenta). (c) Compensation statistic (*CV*) values (gray dots) for stratigraphic thicknesses ranging from 0.5 to 1400 mm for the TDB-10-01 experiment. The 95% envelope for all *CV* data is shown with cyan lines. Median values for *CV* bins that are shown as red squares are the subcompensational bins (bins below H_{min}), the blue circles are the compensational bins (bins H_{min} and above), and the hollow circles are the bins that have been excluded from the fit. The dashed line indicates H_{max}. The gray box corresponds to the 50th–90th percentiles of relief present within the experiment. Topographic data from within one channel width of the edge of the experiment have been excluded from the analysis to eliminate potential edge effects.

CV will be high when the thickness across a chronostratigraphic package is variable or low when the surfaces that define a chronostratigraphic package have similar shape (e.g., Figure 1b). The population of *CV* values over a range of chronostratigraphic windows reflects the morphodynamic history of the landscape. For example, a variable (high *CV*) chronostratigraphic package could result from a highly channelized phase in a delta, and a low *CV* package could result from sheet-flow-dominated deposition (Figures 1a and 1b). When observed over a range of thickness windows, *CV* shows power law decay:

$$CV = a\Delta\overline{\eta}_m^{-\kappa} \tag{2}$$

For uncorrelated random sedimentation—i.e., depositional events occur randomly across a basin in space and time—*CV* decays as a power law with exponent $\kappa = 0.5$. In cases where aggradation occurs evenly across a basin, sedimentation patterns are compensational (i.e., deposition events commonly fill topographic lows), and local sedimentation at any given time largely matches the long-term background sedimentation pattern fairly well. This results in *CV* decaying according to equation (2) with exponent $\kappa > 0.5$, where a value equal to 1.0 would represent perfect compensation. In contrast, situations where sedimentation patterns are clustered

Table 1. Experiment TDB-10-1 Parameters[a]

Duration (h)	78.2
Water discharge Q_w (L/s)	0.4511
Sediment discharge, Q_s (L/s)	0.011
Q_w:Q_s (—)	41
Base-level rise (mm/h)	5
Cross-section location (m from sediment infeed)	2.13
Cross-section thickness (mm)	65
Cross-section width (mm)	1400
Channel depth (mm)	9–14
Channel width (mm)	219.5

[a]Experiment data from *Wang et al.* [2011].

such that there is a tendency for depositional events of similar scale to persist in one area of a basin, *CV* decays with $\kappa < 0.5$. We call κ the *compensation index* [*Straub et al.*, 2009; *Straub and Pyles*, 2012; *Straub and Wang*, 2013].

Because the compensation index is calculated over a range of chronostratigraphic windows, changes in sedimentation patterns at different scales can be detected and compared. Multiple studies have demonstrated that the compensation index is scale dependent, and in experiments there is significant change in stratigraphic organization at the scale equivalent to a maximum channel depth [*Wang et al.*, 2011; *Straub and Pyles*, 2012; *Straub and Wang*, 2013]. In these systems, the compensation index for scales less than a channel depth show "subcompensation" depositional patterns (i.e., $\kappa < 1.0$), and at scales much larger than a channel depth, deposition is organized compensationally (i.e., $\kappa \sim 1.0$). We call this transition between subcompensational and perfectly compensational sedimentation the *compensation scale*; it is hypothesized to mark the transition between deposits which reflect autogenic patterns at small scales and stratigraphy controlled by the allogenic balance of sediment supply and accommodation creation at large scales [*Wang et al.*, 2011; *Straub and Wang*, 2013].

The compensation statistic therefore provides a powerful hypothesis-testing tool to investigate landscape dynamics and allogenic signal preservation in stratigraphy, provided that we can (1) reliably identify the compensation scale in a given system and (2) estimate subcompensation (autogenic) organization accurately. At present, it is untested whether these measures can be accurately quantified and compared in natural systems, particularly given the constraints imposed by the limited extent and resolution of stratigraphic data sets.

2.1. Identifying Autogenic Scales and Organization Using the Compensation Statistic

To explore how the compensation statistic can be used to identify autogenic scales and organization in natural deposits, we leverage stratigraphy generated in a well-constrained, autogenic experiment. The Tulane Delta Basin 10-1 (TDB-10-1) experiment was designed to observe autogenic behavior in a physical experimental delta built in 4.2 m long, 2.8 m wide, and 0.65 m deep experimental basin [*Wang et al.*, 2011; *Straub and Esposito*, 2013; *Straub and Wang*, 2013]. Sedimentation rate, water discharge, and base-level rise were kept constant throughout the run (Table 1). Laser topography scans were acquired every 2 min for the duration of the experiment (78.2 h) with 1 mm horizontal and 0.5 mm vertical resolution. Here we use a flow-perpendicular laser-topography transect 2.1 m from the sediment infeed point (TDB-10-1 M or medial transect in *Wang et al.* [2011] and *Straub and Wang* [2013]; Figure 1a). The compensation statistic (*CV*) was calculated for every possible pair of preserved chronostratigraphic surfaces according to equation (1) (Figure 1b).

Chronostratigraphic-thickness and compensation-statistic data pairs are binned before fitting equation (2). Following best practices for widely scattered data [*Newman*, 2005; *Clauset et al.*, 2009] we use logarithmic bins to group the *CV* values by thickness and use the median *CV* value for each bin to estimate power law relations for the data (equation (2)). In practice, we choose the maximum number of bins that maintains both a relatively smooth 95% envelope and stable bin medians across the thickness ranges of interest (Figure 1c and supporting information). For fitting equation (2), we exclude the first and last bins because they are only partially characterized. In the case of limited instrument or mapping resolution, we also exclude all bins that fall below a minimum cutoff that accounts for incompletely characterized bins at small thickness intervals (supporting information). In the TDB 10-1 data set we chose a cutoff of 1.0 mm because of the resolution limits of the laser-topography measurements.

Identifying the compensation scale can be difficult in a widely scattered *CV* data. Previous compensation analyses of the TDB-10-1 experiment have used chronostratigraphic surfaces based on absolute time [*Wang et al.*, 2011; *Straub and Wang*, 2013], and chronostratigraphic thickness [*Wang et al.*, 2011] has
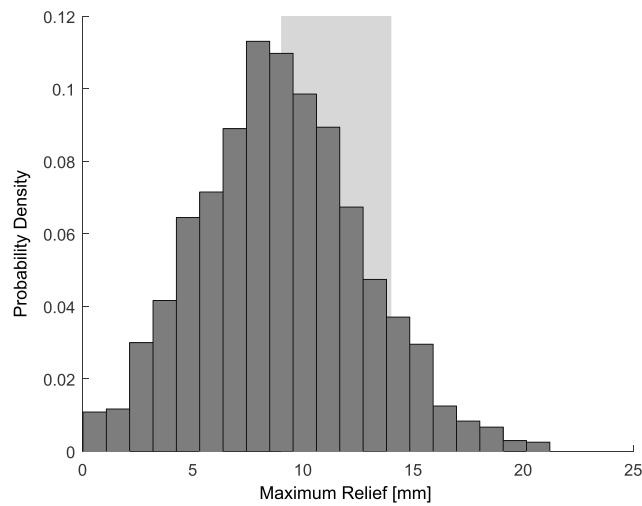
Figure 2. Histogram of the maximum relief measured from every preserved chronostratigraphic surface. The gray box indicates the 50th to 90th percentiles of the maximum relief. Relief was measured from the maximum relief of the preserved topographic surfaces in Figure 1b, excluding the regions within one channel width of the edge of the experiment. Most of the relief on an individual chronostratigraphic surface is from the channel depth, although some relief is due to the larger, convex up trend of the experimental delta surface.

shown that sedimentation patterns shift from random ($\kappa \sim 0.5$) to compensational ($\kappa = 1$) at scales ranging from 9 to 14 mm. This scale range coincides with the characteristic channel scale observed in the experiment, specifically the 50th–90th percentile topographic relief measured in this study (Figure 2 and Table 1). Similarly, in our analysis of preserved stratigraphic surfaces it is difficult to identify one specific scale at which the data become perfectly compensational; rather, there is a range of scales over which sedimentary packages transition from being randomly distributed or clustered to evenly (compensationally) distributed (e.g., at small scales (<5 mm) median CV values yield a $\kappa \ll 1.0$ and at very large scales (>30 mm) $\kappa = 1.0$).

To constrain the minimum extent of this "compensation zone" we identify the smallest scale for which $\kappa = 1.0$ (using a five-point moving window to calculate equation (2); supporting information). This scale—H_{min}—is 7.4 mm for TDB-10-1 stratigraphy. H_{min} is a conservative estimate of the smallest possible window at which the boundary conditions of the basin (i.e., the mass balance of sediment supply and accommodation) may be influencing how sedimentary packages are deposited. Because this estimate is affected by the number of CV points in a data set and data binning (supporting information), it should be considered a heuristic guide for identifying scales that are unequivocally not influenced by mass balance sedimentation, not a definitive scale at which allogenic sedimentation takes over. Consequently, with sufficient data equation (2) fit to scales smaller than H_{min} characterizes autogenic sedimentation patterns in TDB-10-1 ($\kappa = 0.4$ reflecting random or slightly persistent sedimentation patterns; Figure 1).

Another notable characteristic of the compensation statistic analysis of TDB-10-1 is that the range of CV values decreases abruptly around 17 mm; CV values for packages thinner than 17 mm span 4 orders of magnitude, but the range of CV values collapses significantly and remains fairly constant for packages thicker than 17 mm. This scale corresponds closely to the maximum relief observed in experimental topography (17 mm = 97th percentile relief; Figure 2). This indicates that the maximum autogenic relief on the autogenic landscape sets the upper limit of variability in sediment-package thickness within the deposit. Packages thicker than this are generally flatter and are filling the basin evenly. Consequently, the scale at which CV scatter collapses (shown by the "funneling" of the 95% envelope; Figure 1 and supporting information) can be used to estimate the maximum possible scale of autogenic stratigraphy—H_{max}. Although estimating H_{max} is subjective, other more robust ways to estimate it are impractical (for example, a maximum-likelihood-based approach), given that the amount that the CV scatter reduces is highly variable and may depend on the resolution of the data set.

Together, H_{min} and H_{max} can be used to bracket the zone over which the handoff between autogenic and allogenic sedimentation occurs. Observations from this TDB-10-1 analysis are consistent with the hypothesis that the maximum relief across a landscape sets the compensation scale—below which sedimentation patterns are highly variable and reflect intrinsic dynamics in the sedimentary system and above which sedimentation patterns are even reflecting the long-term balance of sediment-supply and accommodation creation in a basin. Compensation-statistic analysis of TDB-10-1 stratigraphy yields a compensation scale range that is within 20% of the modal and maximum channels observed in the experiment.

3. Effects of Data Set Resolution on Autogenic Scales and Organization Estimates

Even the best characterized data sets from natural deposits are significantly lower resolution and smaller in extent than what is available for experiments. In order to compare across multiple systems, and between experimental and field data sets, it is useful to scale the extent of stratigraphic exposures to the characteristic scale of formative elements of the depositional system (e.g., channel-element width and thickness in fluvial-deltaic systems [e.g., *Wang et al.*, 2011] or lobe dimensions for deepwater fans [e.g., *Straub and Pyles*, 2012]). Some of the best exposed fluvial-deltaic outcrop belts show continuous exposure that reaches up to 5 times the width and 10 times the thickness of a typical channel deposit [e.g., *Mohrig et al.*, 2000; *Olariu and Bhattacharya*, 2006; *Pranter et al.*, 2009; *Enge et al.*, 2010; *Fielding*, 2010; *Schomacker et al.*, 2010; *Olariu et al.*, 2012; *Bhattacharyya et al.*, 2015]; however, many field exposures of ancient fluvial-deltaic deposits are much more limited and subsurface (seismic or well) data sets typically have low vertical (thickness) resolution, limited spatial extent, or both.

To explore how data set extent and resolution may influence the degree to which compensation scale and subcompensation organization can be characterized, we subsampled TDB-10-1 experimental data and recalculated compensation-scale and compensation index values for a series of restricted extent and resolution data sets. The entire TDB-10-1 experiment is approximately 10 times wider and 27 times thicker that the dimensions of the 90th percentile channel (Figure 1 and Table 1); we restricted our analysis to the portions of the experiment that are at least one-channel-width away from the edge of the experiment to limit potential edge effects. We randomly selected portions of the data set that range from 2 to 12 times the channel depth and 1 to 10 times the channel width (locations in Figure 3 and results in Figures 4–6). Additionally, we extracted every second and fifth surfaces from one subsampled data set to represent high-and low-resolution outcrop mapping (Figure 7). Using the approach for data aggregation outlined in the section 2.1 we estimated H_{min} from each subsampled data set by locating the minimum chronostratigraphic bin that maintained a compensation index of $\kappa = 1$ and estimated the subcompensation index by fitting equation (2) to the remaining (smaller) bin medians (Figures 4–6). In cases where no range of chronostratigraphic thicknesses yielded a compensation index of $\kappa = 1.0$, we considered H_{min} undetectable. H_{max} was estimated as the bin center that coincided with the end of the *CV* scatter-reduction zone (often highlighted by the transition from a wide, funnel-shaped to a parallel 95% envelope; Figures 4–6). As a reference we use results from analysis of the full data set (Figure 4a), which yielded $H_{min} = 7.4\,mm$, $H_{max} = 17.0\,mm$, and a subcompensation index of $\kappa = 0.4$.

3.1. Data Set Extent

All subsamples of the full TDB-10-1 data set yield H_{max} values of 17–20 mm. Regardless of whether data sets were reduced in width or thickness, the abrupt decrease in *CV* variability consistently reflects the highest range of topographic relief observed on the experimental delta, between the 95th and 99th percentiles. This range is fairly precise, given that each data set has different numbers of surfaces, different thickness ranges, and slightly different data-binning divisions (supporting information). This demonstrates that the maximum autogenic scale may be observable as an abrupt reduction in *CV* even in stratigraphic data sets that are relatively thin or narrow.

Some data sets failed to produce $\kappa = 1.0$ over any stratigraphic thickness ranges (Figures 4n, 4s, 4x, 4j, and 4y). These data sets tend to be thin (≤3 channel depths), but other data sets similar in thickness did yield $\kappa = 1.0$ (e.g., Figure 4t). Similarly, H_{min} values are less consistent than H_{max} estimates, ranging from 3 to 10 mm. (The 50th percentile channel depth in the experiment was 9 mm.) Furthermore, subcompensation index values for the reduced-scale data sets varied widely from $\kappa = 0.1$ to 0.8. This uncertainty is only in part due to the numerical sensitivity of identifying H_{min} and κ over small scales (supporting information); it may also reflect different dominant autogenic sedimentation patterns present locally within the subsections of the experiment.

Replicate subsamples of the same width and thickness show similar consistency among H_{max} estimates, variability in H_{min} estimates, and widely ranging κ values (Figures 5 and 6). For stratigraphic samples the size of relatively large outcrops (12 channel-depths thick by three channel-widths wide, comparable to the fluvial outcrops presented below; Figure 5), H_{max} estimates range from 15 to 20 mm, H_{min} estimates range from 3 to 7 mm, and κ values range from 0.3 to 0.7. These data sets are all the same size, so they have the same number
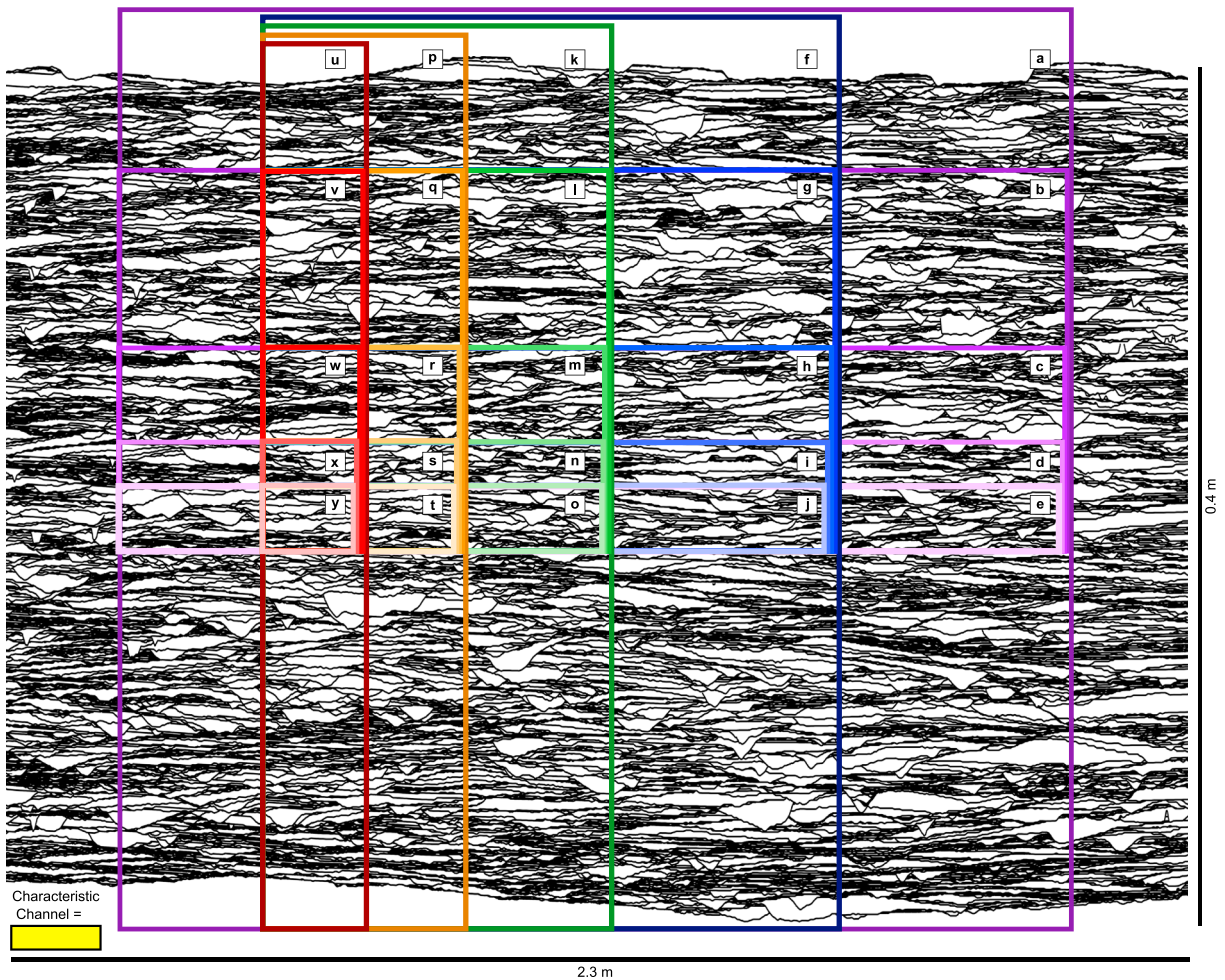
Figure 3. Location of the data sets used in Figure 4. Note that the boundaries have been shifted slightly to indicate that the data sets are nested. The characteristic channel is 14 mm deep (the 90th percentile relief) and 220 mm wide.

of surfaces and rely on the same binning scheme. However, qualitatively, each subsample has different characteristic architectures, particularly with respect to the abundance and distribution of channel- or sheet-like deposits (Figure 5a). For example, Figure 5g has stratigraphic intervals extending across the plot width that are dominated by channels (low in the section) and sheets (middle of the plot), Figure 5d appears to have clusters of channels interspersed vertically and laterally with patches of sheet-like deposition, and Figure 5c has a more random-looking mix of channels and sheets. These local differences in architecture may be reflected in the subcompensation index κ values (e.g., where $\kappa = 0.6$ for Figure 5g may be indicating fairly even autogenic sedimentation, $\kappa = 0.3$ for Figure 5d may indicate persistent or clustered autogenic sedimentation). Similar variability is seen in data sets that approximate smaller outcrops (three channel-depths thick and only one channel-width wide, similar to the delta outcrops presented below; Figure 6). Here again, $H_{\max}$ (12–18 mm) is consistent with other estimates for TDB-10-1, and plots that produce vastly different subcompensation index κ values appear to have different architectures. Collectively, the ensemble average of κ measured in the subsamples approximates the estimate obtained from the full data set. This underscores the possibility that small outcrops may reflect primarily the local manifestation of autogenic sedimentation, but that by making the same measurements in a number of outcrops spread across a basin, it may be possible to reconstruct the basin-wide average autogenic sedimentation patterns.

3.2. Data Set Resolution

The resolution of a subsampled region does not appreciably change the estimate of the compensation scale until the smallest resolved thicknesses are larger than the compensation scale (Figure 7). The primary
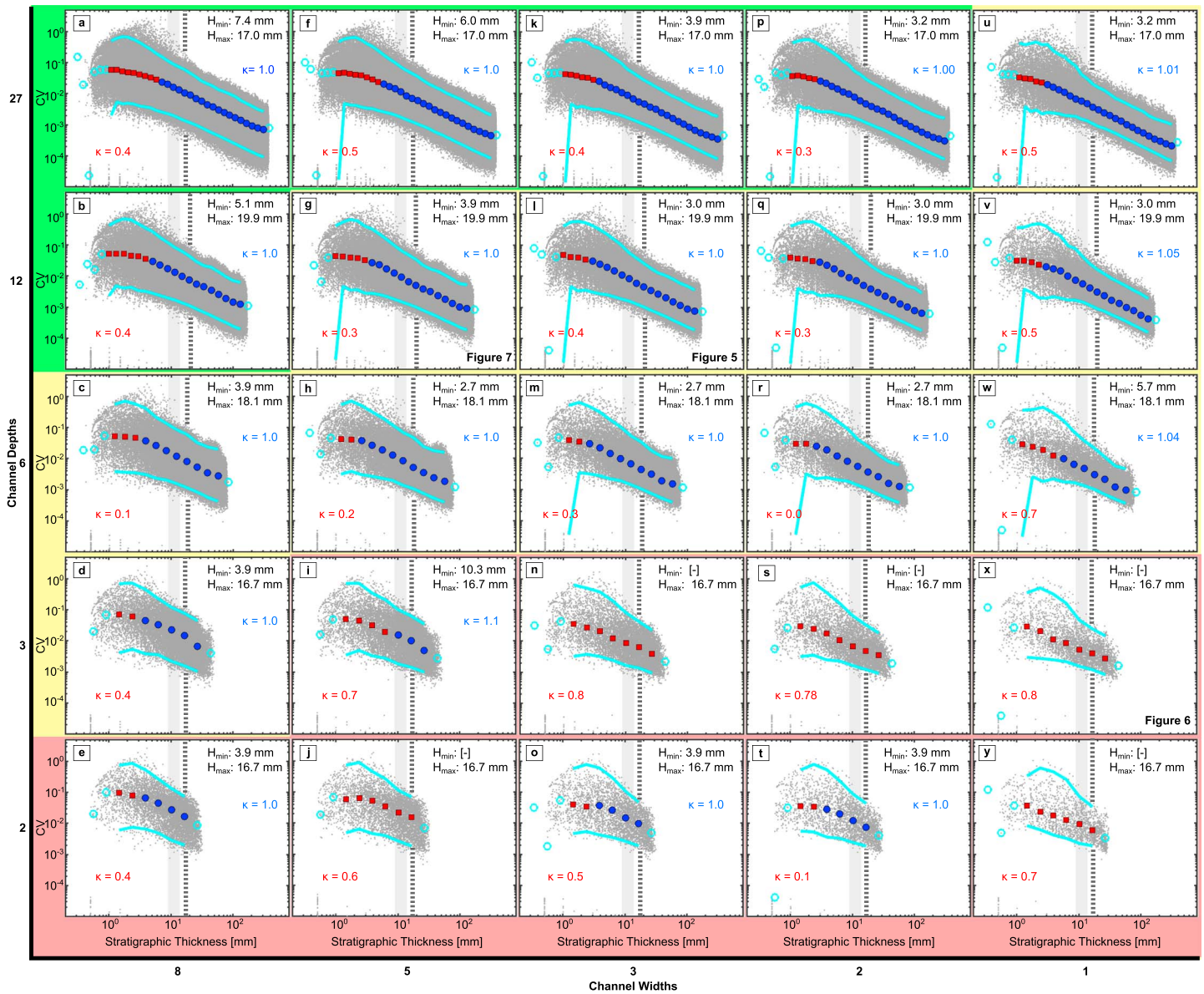
Figure 4. Compensation statistic (*CV*) plots of the subsampled TDB-10-01 stratigraphic data sets scaled by the experimental channel scale (e.g., Figure 1b) arranged in rows of decreasing thickness from top to bottom and columns of decreasing width from left to right, with the full TDB-10-01 data set from Figure 1 shown in A. The annotations and colors are the same as in Figure 1. Subsampled data sets that are shown again in Figures 5–8 are indicated. The background shading on the figure indicates the degree to which the sample of the data set reflects the system-wide scale and organization: green demonstrates the system-wide behavior, red demonstrates the local behavior, and yellow are the systems that could be heavily influenced by local effects.

consequence of reduced data set resolution is that there are simply fewer chronostratigraphic packages resolvable at small mean thicknesses, so the density of *CV* values increases with chronstratigraphic thickness (Figure 7; in contrast to the large number of *CV* pairs at small mean thicknesses in Figure 7a). In general, reducing the number of resolvable surfaces in an outcrop can lead to misestimating the subcompensation index, as it may be poorly constrained because of a lack of data at small scales, but does not significantly change the compensation scale until there are too few surfaces mapped below the compensation scale to fit any subcompensation index. Because the compensation statistic robustly reconstructs compensation scale, even in relatively low-resolution data sets, it can successfully be applied to many different types of stratigraphic data (e.g., well logs, ground penetrating radar (GPR), or seismic surveys) provided that the minimum resolution of chronostratigraphic packages is smaller than the expected compensation scale.
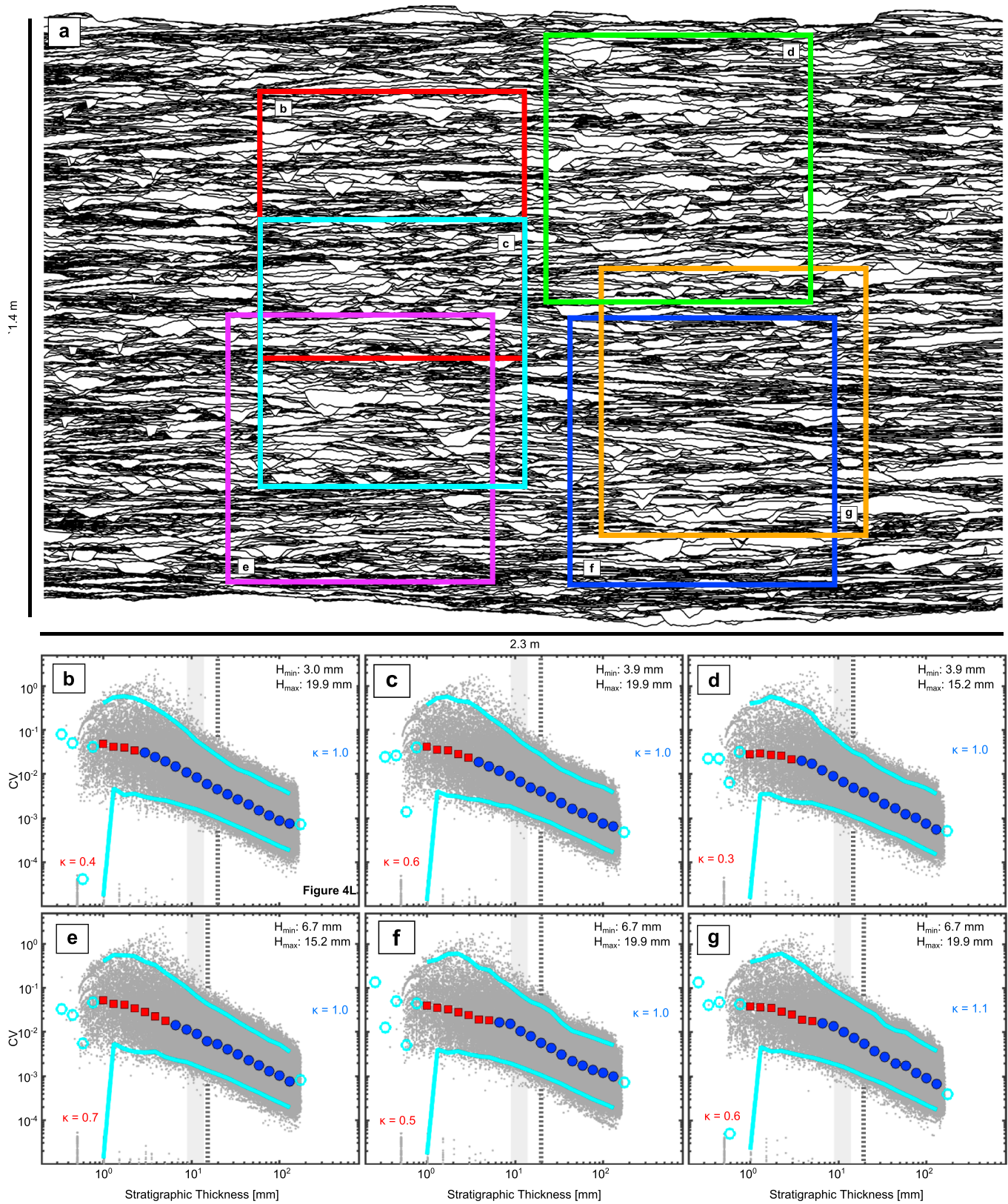
Figure 5. Replicates of samples with the same dimensions as Figure 4l. Replicates estimate H_{min} between 3.0 and 6.7 mm and a H_{max} between 15.2 and 19.9 mm, compared to the 7.4 and 17.0 mm measured in the largest sample (Figure 1c). The extent of these samples is roughly equivalent to the extent of the lower Williams Fork Formation data set.
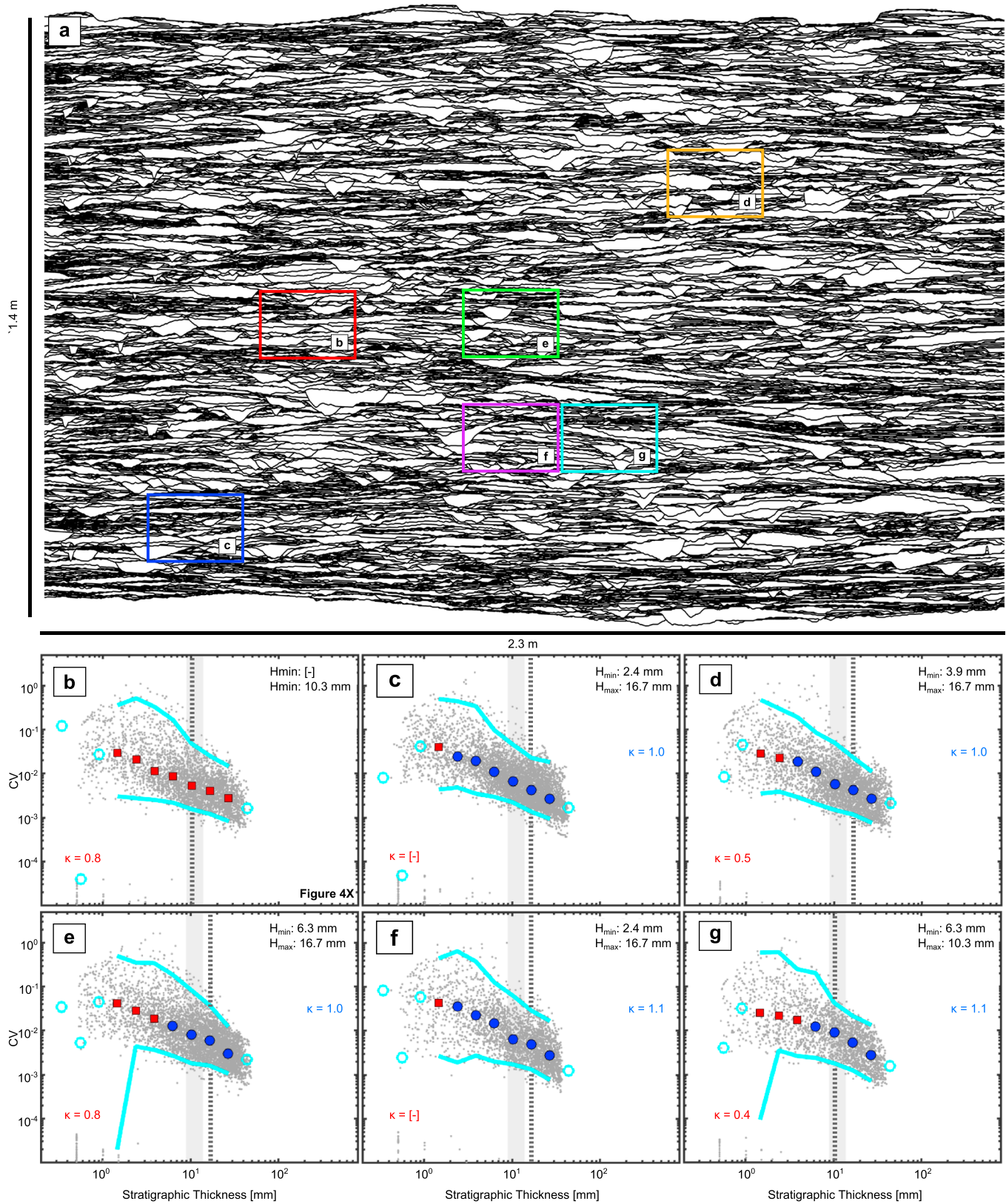
Figure 6. Replicate samples of the Figure 4x sample. Estimates of H_{min} are 2.4–6.3 mm and the H_{max} are 10.3–16.7 mm, compared to the 7.4 and 17.0 mm of the largest sample (Figure 1c). For a minority of sample, a compensation scale cannot be determined (e.g., b). The extent of these samples is likely similar to that of the lower Ferron Sandstone data set.

3.3. Implications

Data quality can be partially inferred from compensation plots. Data sets that are sufficiently wide and thick will have enough bins to resolve two power law regions on the plot: one subcompensation $\kappa < 1.0$ relationship and one, where $\kappa = 1.0$, that defines the thickness scales over which chronostratigraphic packages are evenly (i.e., compensationally) deposited. If a data set is not thick enough, the compensation index will be below $\kappa = 1.0$ (e.g., Figures 4j, 4n, 4s, 4x, and 4y). If a data set is too narrow, the subcompensation bins may not fit a power law relationship well (e.g., the relation will look curved or nonlinear on the log-log CV plot). An outcrop that has full resolution will have an even, dense pattern of CV pairs across all chronostratigraphic windows (e.g., Figures 1 and 7a), and an outcrop that is partially resolved will show limited point density for small chronostratigraphic windows (e.g., Figures 7b and 7c).

Overall, these results suggest that compensation-scale estimates are quite robust for most stratigraphic data sets. H_{max} consistently corresponds to the large tail of the distribution of relief on the delta surface and is insensitive to data set precision as long as the minimum usable bin is smaller than the compensation scale. These results also show that limitations on data set extent or resolution are unlikely to show compensation scales that are artificially large; when a compensation scale is detected in a given data set (i.e., there is a range of chronostratigraphic thicknesses for which $\kappa = 1$), that scale is likely to be within a factor of 2, if not within 50% of the actual maximum autogenic scale of a given system.

Interpreting autogenic sedimentation patterns using the subcompensation index can be complicated because for small data sets, system behavior may only be partially sampled and an individual data set is likely to show local organization, not the average autogenic behavior of the system. It may be possible to ascertain the characteristic autogenic behavior of a system using a large number of limited-extent or limited-resolution observations from a given system (e.g., multiple discontinuous outcrop belts or multiple well-log or core cross sections), although currently, it is not clear how sampling variability and data set resolution interact and define uncertainties associated with subcompensation-index estimates.

These results underscore the importance of estimating data set size relative to the size of characteristic depositional elements within a given system. This can be challenging because we may not know what type of landforms are driving compensational sedimentation patterns—and thus setting the scale of autogenic stratigraphy—in different landscapes or seascapes. *Wang et al.* [2011] propose that the compensation scale should approximate the maximum topographic relief that can develop in a particular environment. In channelized landscapes (e.g., fluvial, deltaic, and deepwater systems), it is reasonable and useful to use the channel scale as a null estimate of the compensation scale for designing mapping campaigns and for evaluating and comparing compensation-statistic results.

4. Identifying Autogenic Scales and Organization in Ancient Fluvial and Deltaic Deposits

The compensation statistic is a useful tool for identifying the upper limit of autogenically driven sedimentation patterns in a depositional system and can provide insight into the nature of self-organized depositional patterns in different environments. This information is necessary for stratigraphers to answer key outstanding questions about landscape dynamics in sedimentary systems including (1) what controls the maximum autogenic scale in a given setting and (2) the degree to which autogenic sedimentation patterns are random or organized over long time scales.

Using insight from analyzing TDB-10-1 subsampled data sets of limited extent and resolution, we demonstrate how the compensation statistic may be applied to outcrop data of ancient fluvial and deltaic deposits. We evaluate four data sets—two fluvial and two deltaic—that exemplify outcrops with extensive and high-quality exposures and span a range of scales and resolutions relative to their formative depositional systems (Table 2). This set of four case studies shows how outcrop extent, mapping, and data quality may influence the detectability of the compensation scale and subcompensation organization and highlights how this approach may be used to understand controls on autogenic dynamics in ancient systems.

4.1. Fluvial Case Studies

Recent work has highlighted the possibility that some fluvial systems may be self-organized on relatively long temporal and spatial scales. Studies in several fluvial systems using a variety of statistical approaches
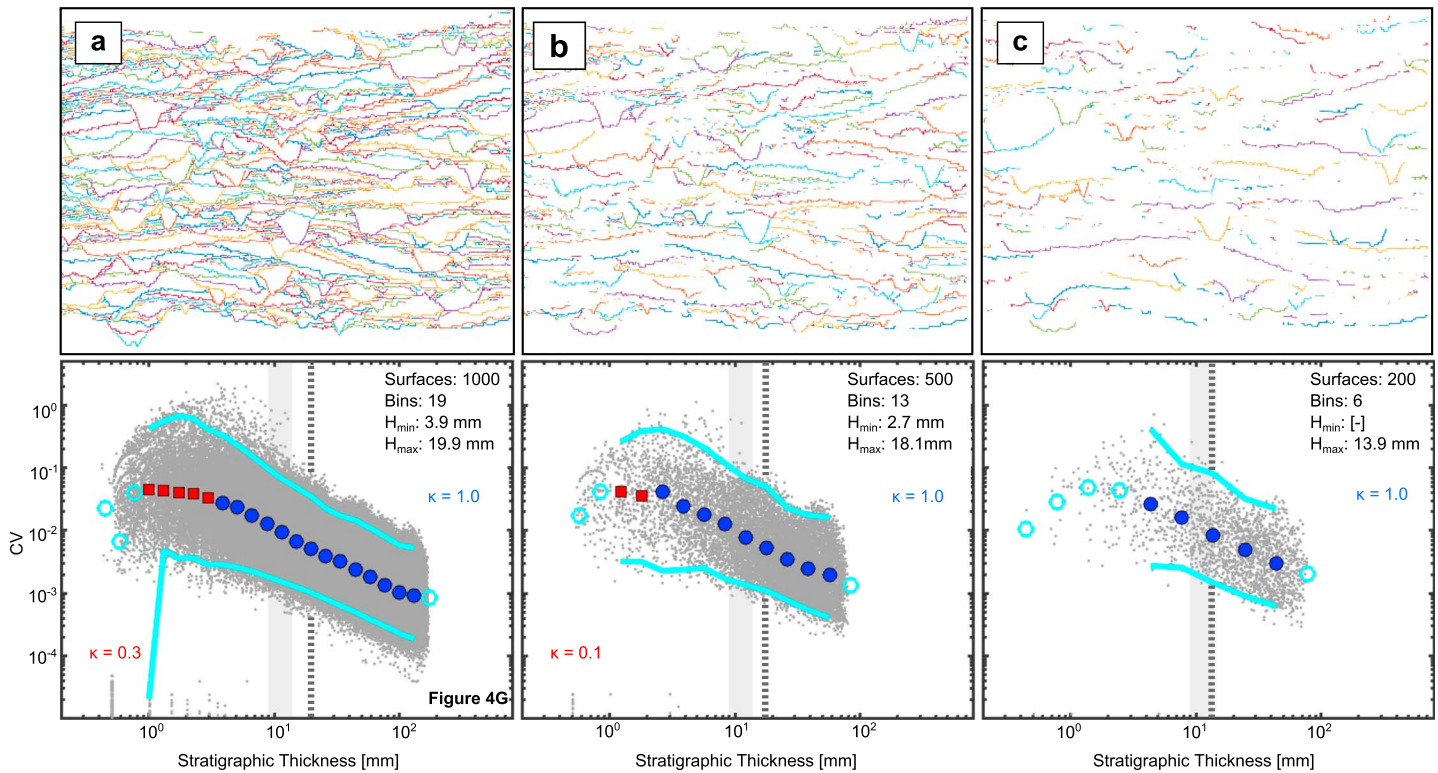
Figure 7. Compensation statistic (*CV*) plots of downsampled TDB-10-1 subsamples (Figure 4g). The annotations and symbols that are the same as in Figure 1b have half the number of chronostratigraphic surfaces as the original subsamples *a* and *c* have 1/5 the number of chronostratigraphic surfaces as the original. Samples *a* and *b* have similar compensation scales, but the subcompensation indices differ. Sample *c* does not have enough surfaces below the compensation scale to determine the compensation scale or the subcompensation index. The extent of these samples is similar to the Ferris Formation data set.

have shown that intrinsic avulsion dynamics may produce random or organized basin-filling sedimentation patterns [*Hajek et al.*, 2010; *Jerolmack and Paola*, 2010; *Hofmann et al.*, 2011; *Wang et al.*, 2011; *Flood and Hampson*, 2015; *Chamberlin et al.*, 2016]. In light of these results and remaining outstanding questions about fluvial avulsion dynamics, it is important be able to detect and estimate both the nature of and scale over which autogenic sedimentation patterns occur with methods that allow meaningful comparisons among natural systems and between outcrop and experimental results. To demonstrate how the compensation statistic may be used practically in pursuit of answers to these questions, we present outcrop-based analyses of ancient sedimentation patterns in the Ferris Formation (Cretaceous/Paleocene, Hanna Basin, Wyoming) and the Williams Fork Formation (Upper Cretaceous, Piceance Basin, Colorado).

4.1.1. Ferris Formation

The Ferris Formation was deposited as a rapidly aggrading upland fluvial system draining Laramide uplifts in the Late Cretaceous and Early Paleogene, filling the Hanna Basin, Wyoming [*Weimer*, 1984; *Lillegraven et al.*, 2004; *Hajek et al.*, 2012]. The Ferris Formation exposure in the northern Hanna Basin is steeply dipping, exposing a stratigraphic cross section (orthogonal to mean paleoflow direction) across the present-day land surface (Figure 8a). Ferris rivers were 0.3–0.9 m (mean = 0.59 m) deep, as measured by bar clinoforms (Figure 8b), and deposited single-story and multistory sand bodies ranging from 1 to 10 m thick (mean = 4.4 m) and 10 to 900 m (mean = 162 m) wide [*Hajek et al.*, 2012]. Individual channel-belt deposits were mapped with differential GPS across a 1700 m wide by 250 m thick study area [*Hajek et al.*, 2010]. Chronostratigraphic surfaces ($n = 119$) were constructed by projecting pseudo-horizons laterally away from channel body rectangles that represent the maximum thickness and width of each channel-belt sand body (Figure 8c) [*Wang et al.*, 2011]. This strategy for mapping chronostratigraphic surfaces captured paleo-topography larger than 2 m. The full data set represents a stratigraphic package that is more than 50 times thicker and 10 times wider than the average Ferris channel-belt sand body.

Table 2. Characteristics of the Case Studies

| Unit	Depositional Environment	Channel-Belt Width (m)	Channel Depth (Sand Body/ Parasequence Thickness; m)	Width (m)	Thickness (m)	Number of Surfaces	Mapping Scale (Minimum Resolution; m)	Citations
Ferris Formation	Fluvial	10–900, mean = 162	0.3–0.9, mean = 0.59 (1–10, mean = 4.4)	1700	350	119	Channel belt	*Hajek et al.* [2010, 2012] and *Wang et al.* [2011]
Williams Fork Formation	Fluvial	20–380, mean = 90	1.0–3.7, mean = 2.5 (1.9–11.9, mean = 4.7)	1500	200	67	Channel belt	*Cole and Cumella* [2005], *Pranter et al.* [2009], and *Chamberlin et al.* [2016]
Sego Sandstone	Deltaic	~150	2–5 (10–20)	300	25	271	Bed set	*Willis* [2000] and *Willis and Gabel* [2001]
Ferron Sandstone	Deltaic	225–150	3.9–5.2 (10–20)	150	45	82	Bed set	*Corbeanu et al.* [2004]

Compensation statistic (*CV*) values for the Ferris Formation were calculated over a range of 2–200 m. *CV* points were aggregated into 17 logarithmic bins; the largest bin and the bins smaller than 3 m were excluded (Figure 8d). The density of *CV* points increases after the compensation scale. H_{min} and H_{max} both appear to be at the bin centered at 30.7 m. The "funneling" or scatter reduction in *CV* values also appears complete at the bin centered at 30.7 m. The subcompensation index is 0.8, estimated over chronostratigraphic thicknesses between 2.5 and 21.2 m.

All evidence suggests that the compensation scale for the Ferris Formation is much larger than the channel depth. Both the numerically defined H_{min} and the qualitative H_{max} indicate that the compensation scale is around 30.7 m. Although it is extensive, the Ferris Formation data set is fairly low resolution. Our results from downsampling TDB-10-1 data show that the low resolution of the Ferris Formation data set is not likely to artificially increase the compensation scale. The compensation scale is at least 30 times the maximum flow depth observed in *Hajek et al.* [2012] and more than 3 times the average sand body thickness. The Ferris Formation data are likely too poorly resolved to accurately determine the subcompensation index. Sparse *CV* points below ~10 m indicate low resolution (e.g., Figures 7c and 7d). Similarly, the muted funneling of the *CV* ranges in subcompensation bins also indicates that sedimentation patterns over small chronostratigraphic thickness windows are not well characterized.

Wang et al. [2011] estimate subcompensation organization using a slightly different data-handling and binning approach and obtain $\kappa = 0.5$. *Hajek et al.* [2010] use spatial point process statistics to show that channel belt deposits are statistically clustered in the same stratigraphic plot (this would correspond to $\kappa < 0.5$). Given the lack of resolution over this critical subcompensation window, the subcompensation index of this data set is unreliable.

4.1.2. Williams Fork Formation

The Williams Fork Formation was deposited in a lowland river system draining the Sevier highlands and filling the Piceance Basin in the Late Cretaceous and comprises a mud-dominated lower member (the subject of this study) and a sand-dominated upper member [e.g., *Cole and Cumella*, 2005; *Pranter et al.*, 2009]. An extensive and well-studied outcrop belt of the lower member is exposed in Coal Canyon near Palisade, Colorado. Coal Canyon exposes a cross section 1500 m wide and 200 m thick of the lower Williams Fork Formation oriented orthogonal to mean paleoflow direction in *Pranter et al.* [2009] (Figure 9a). Paleoflow depths measured from bar clinoforms are 1.0–3.7 m (mean = 2.5 m), and sand body dimensions range from 1.9 to 11.9 m (mean = 4.7 m) thick and 20–380 m (mean = 93 m) wide in the study area (Figure 9b) [*Cole and Cumella*, 2005; *Pranter et al.*, 2009; *Chamberlin et al.*, 2016]. Using terrestrial lidar scans, chronostratigraphic surfaces (*n* = 67) were mapped at the bases of channel belts, with flat pseudo-horizons projected across
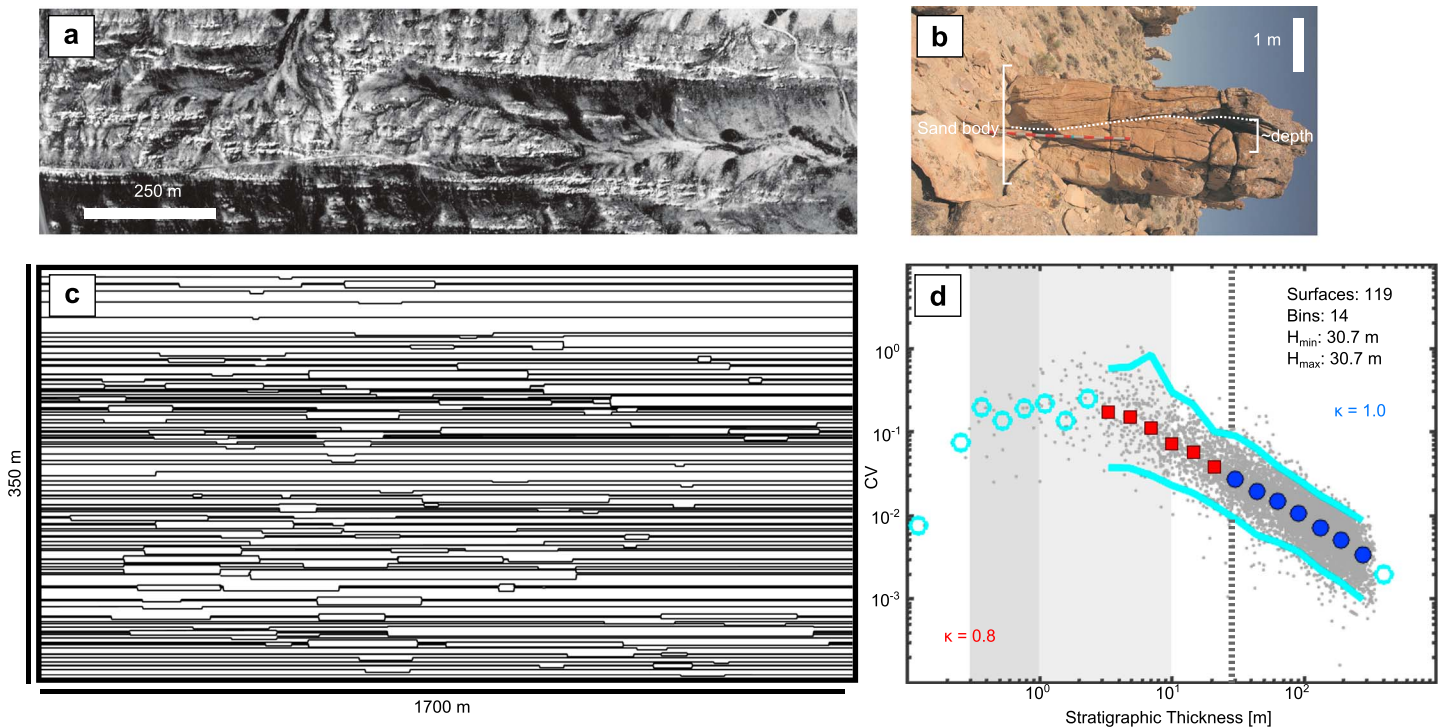
Figure 8. (a) Airphoto of the Ferris Formation outcrop in the Hanna Basin, Wyoming (supporting information). The white areas are the sand bodies. Outcrop is 1700 m wide and 350 m thick. Flow is into the ground; stratigraphic up is to the top of the photo. (b) Field photograph of a representative channel sandstone in the Ferris Formation. The photo has been rotated so that stratigraphic up is to the top of the photo; paleoflow direction is to the left, into the ground. The bar clinoforms can be seen at the top of the sand body dipping down to the left. The height of these clinoforms (dashed white line) indicates a paleoflow depth around 1 m. Dune cross stratification in the top left of the sand body is 15–30 cm height, which is also consistent with flow depths ~1 m. (c) Chronostratigraphic surfaces (119) for the Ferris Formation outcrop were constructed with horizontal pseudo-horizons projected through the floodplain and rectangles representing the maximum width of a channel and the mean sand body thickness. Pseudo-horizons were clipped to represent only preserved surfaces. (d) Compensation statistic (*CV*) plot of the Ferris Formation. The density of *CV* points increases significantly across the subcompensation bins, and the reduction in scatter evident in the 95% envelope is not pronounced. We had to exclude bins smaller than 3 m due to the scarcity of data within those bins. The annotations and colors are the same as in Figure 1.

floodplain deposits (Figure 9c) [*Chamberlin et al.*, 2016]. These surfaces were projected onto a 2-D plain orthogonal to mean paleoflow direction and corrected for a gentle regional tectonic dip (Figure 9c). Channel belts thicker than 1 m are resolved within this data set. The entire data set is 15 times wider and 50 times thicker than the average channel-belt sand body.

Compensation statistic (*CV*) values for the lower Williams Fork Formation were calculated over a range of 4–150 m. All *CV* points were aggregated into 15 logarithmic bins; the largest bin and bins smaller than 4 m were excluded (Figure 9d). The density of *CV* points increases near the compensation scale. H_{min} is at the bin centered at 12.1 m and H_{max} at the bin centered at 17.3 m. The subcompensation index is 0.7, estimated over chronostratigraphic thicknesses between 2.1 and 12.1 m.

Like the Ferris Formation, the compensation scale of the lower Williams Fork is much larger than the range of channel depths. The compensation scale is over 3 times the largest paleoflow depth reported but less than 2 times the largest sand body scale. The sparse points at stratigraphic thicknesses <12 m on the compensation plot and the muted funneling of the 95% envelope both indicate low resolution (e.g., Figures 7c and 7d). This means that the lower Williams Fork Formation outcrop is likely too poorly resolved to confidently determine subcompensation behavior using the compensation statistic.

4.1.3. Comparison of Fluvial Case Studies
Both fluvial case studies use data sets of large extent but low resolution. From our downsampling experiments, both systems are large enough to enable system-wide characterization. However, the resolution at which they were mapped does not enable us to characterize their subcompensational organization using the compensation statistic. *Chamberlin et al.* [2016] conducted a compensation statistic analysis using slightly different binning strategy; they estimated the subcompensation index as 0.5, but this value was heavily
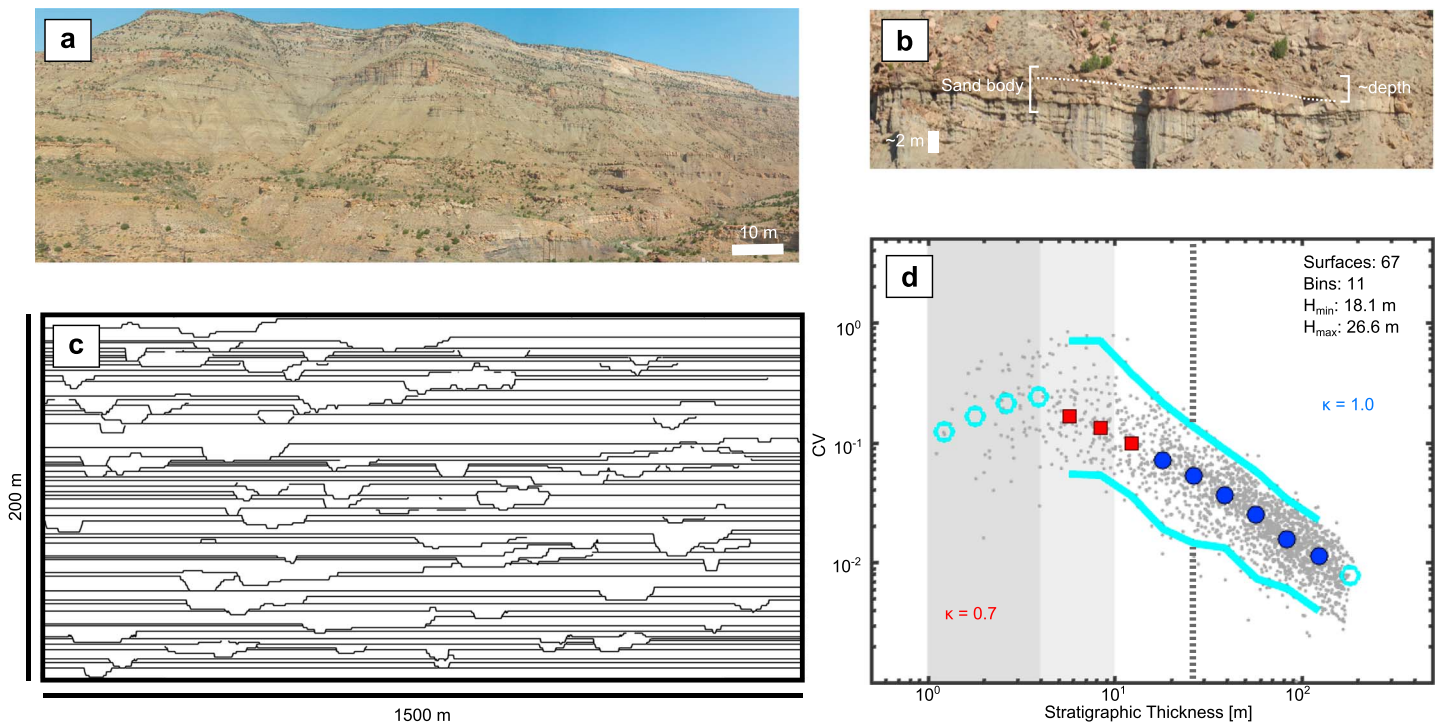
Figure 9. (a) Field photo of the lower Williams Fork Formation outcrop exposed in Coal Canyon, Colorado (supporting information). Channel sand bodies are the resistant units in the hillside. (b) Field photograph of a representative channel sandstone in the lower Williams Fork Formation. The height of the bar clinoforms dip down to the right (dashed white line) indicates a paleoflow depth less than 3 m deep. The depth of the scour at the base of the sand body also indicates a relatively shallow flow. (c) Chronostratigraphic surfaces (67) for the Williams Fork Formation. Base of channels were mapped on a digital outcrop model, and pseudo-horizons were projected through floodplain deposits. Pseudo-horizons were clipped to represent only preserved surfaces. (d) Compensation statistic (CV) plot of the Williams Fork Formation. Note the overall low density in CV points that increases at larger stratigraphic thicknesses. We had to use a large minimum cutoff value of 4 m because of the scarcity of CV values in smaller bins. The annotations and colors are the same as in Figure 1.

dependent on the minimum bin that was included in the analysis [e.g., *Chamberlin et al.*, 2016, Figure 8]. Our analysis of low-resolution data sets in section 3.2 determined that the subcompensation bins become unreliable with low-resolution data sets, such as the lower Williams Fork and Ferris Formation data sets (supporting information). In these cases, autogenic sedimentation patterns are better characterized by other statistical approaches. One such approach is the *k*-function, which has demonstrated that channel bodies within the Ferris are indeed clustered [*Hajek et al.*, 2010]. Similarly, independent analyses of the channel centroids and the probability of multistoried sand bodies both indicate that the lower Williams Fork has spatially uncorrelated (random) sedimentation [*Chamberlin and Hajek*, 2015; *Chamberlin et al.*, 2016]. While the low resolution of the data sets limits the utility of the subcompensation indices, from our downsampling experiments, the compensation scales should still represent the regional compensation scale within a factor of 2.

The compensation scales of the Ferris Formation and the lower Williams Fork Formation indicate that there was topographic relief larger than a channel depth present in both systems. The Ferris Formation compensation scale was at least 30 times as large as the maximum reported channel depth. The lower Williams Fork compensation scale was at least 5 times as large as the maximum reported channel depth. It is unlikely that the reported channel depths are incorrect since channel depth in both systems is well constrained by multiple lines of evidence, including the bar clinoform height, thickness of the abandonment facies (the "mud plug"), and the height of dunes and cross bedding. Additionally, the Ferris Formation compensation scale is over 3 times larger than the largest sand body thickness but the lower Williams Fork compensation scale is less than 2 times as large. Sand body thickness is likely heavily influenced by channel reoccupation events, levee aggradation, and alluvial ridge development [e.g., *Mohrig et al.*, 2000; *Farrell*, 2001; *Tornqvist and Bridge*, 2002; *Chamberlin and Hajek*, 2015; *Edmonds et al.*, 2016]. Larger sources of relief in aggradational fluvial systems include the development of megafans [*Jones et al.*, 2002; *Leier et al.*, 2005; *Hartley et al.*, 2010; *Weissmann et al.*, 2010].

The development of features like alluvial ridges and megafans are all dependent on sediment cohesion, which is a variable that is frequently omitted from experimental deltas, including the experiment we use here [*Hoyal and Sheets*, 2009]. Since both the Ferris and Williams Fork Formation have significant proportions of fine-grained deposits, they likely had enough cohesion to build relief larger than the depth of a channel scour. The differences in compensation scale relative to sand body thickness suggest that where the Ferris Formation may be controlled by some larger source of relief (such as the development of a megafan), the Williams Fork Formation can be explained by normal alluvial ridge development. This also has implication for the lateral scales of both systems: outcrops within the Williams Fork Formation should be scaled to the width of the alluvial ridge, but the width of outcrops within the Ferris Formation might be scaled to the width of a much larger depositional element, potentially to the width of a megafan.

4.2. Deltaic Case Studies

The degree to which deltaic deposits reflect landscape processes, sediment supply from the hinterland, or basinal forces is an important question in sedimentary geology. For example, it is unclear whether sea level or basin depth is the primary control on scales of deltaic packages (e.g., parasequences) or if autogenic organization can play a role [*Sheets et al.*, 2002; *Hoyal and Sheets*, 2009; *Martin et al.*, 2009; *Edmonds et al.*, 2011a; *Wang et al.*, 2011]. Additionally, if landscape dynamics are a prominent control on sedimentation patterns in deltaic deposits, the role of waves, tides, and fluvial processes should result in different styles of autogenic organization [*Bhattacharya and Giosan*, 2003; *Dalrymple and Choi*, 2007; *Jerolmack and Swenson*, 2007; *Ashton and Giosan*, 2011; *Leonardi et al.*, 2013; *Nienhuis et al.*, 2013]. Here we use the compensation statistic in two well-constrained deltaic deposits from the Cretaceous Western Interior Seaway (U.S.)—one interpreted as tide dominated and the other interpreted as being river dominated—to evaluate how compensation scale and autogenic organization differs between the systems.

4.2.1. Sego Sandstone

The Sego Sandstone (Campanian) is a member of the Mancos Shale and was a an eastward prograding, tide-dominated delta building into the Western Interior Seaway [e.g., *Willis*, 2000; *Willis and Gabel*, 2001, 2003]. The studied outcrop of lower Sego Sandstone ("Sandstone 2" of *Willis and Gabel* [2001]) is located in San Arroyo Canyon near the Utah-Colorado border and is oriented slightly oblique to paleoflow (Figure 10a). The outcrop contains primarily tidal bar and distributary channel deposits; as much as possible, we chose this outcrop to avoid areas which may have been scoured by genetically unrelated, incised valleys [*Willis and Gabel*, 2003]. We collected terrestrial lidar scans of the outcrop and mapped chronostratigraphic surfaces from digital outcrop models generated from the lidar scans. Additionally, we estimated channel dimensions of 150 m wide and 2 m deep from channel clinoform thicknesses measured with a laser rangefinder in the field and measured on the digital outcrop model (Figure 10b). Chronostratigraphic surfaces ($n = 271$) were mapped at bed-set boundary scale, with bed sets larger than 20 cm resolved with confidence. Surfaces were projected onto a 2-D plane-parallel to the outcrop exposure, which is within 10° perpendicular to regional paleoflow direction (Figure 10c). Surfaces are discontinuous. The outcrop is over 10 times thicker and 2 times wider than individual channel elements.

Compensation statistic values for the lower Sego Sandstone were calculated over a range of 0.2–15 m. All CV points were aggregated into 17 logarithmic bins; the largest bin and bins smaller than 0.2 m were excluded (Figure 10d). The density of CV points increases slightly near the compensation scale, but in general, the field of CV values is quite dense over the entire stratigraphic-thickness range. Fitting equation (2) reveals that the H_{min} is at the bin centered at 1.9 m; H_{max} is at the bin centered at 6.4 m. The subcompensation index is 0.3, estimated over chronostratigraphic thicknesses between 0.2 and 1.2 m.

The lower Sego Sandstone outcrop shows compensation at a scale consistent with observed channel paleoflow depths. The subcompensation index of the lower Sego Sandstone is well characterized by the high-resolution mapping of chronostratigraphic packages much smaller than the compensation scale. The subcompensation index demonstrates strongly persistent autogenic behavior. While the subcompensation index value artificially due to poorly characterized subcompensation bins, the strong power law fit is inconsistent with the weak power law fits observed in the experiments with an artificially reduced subcompensation index value.
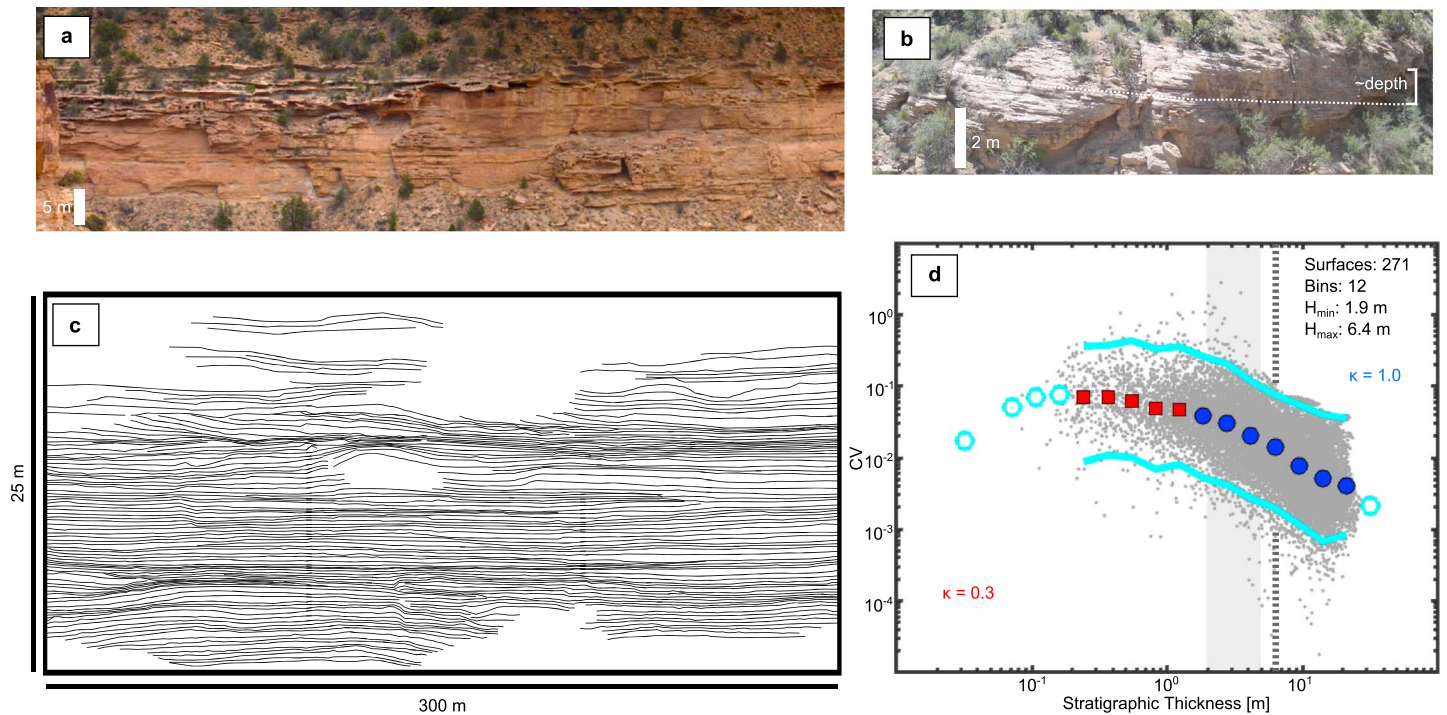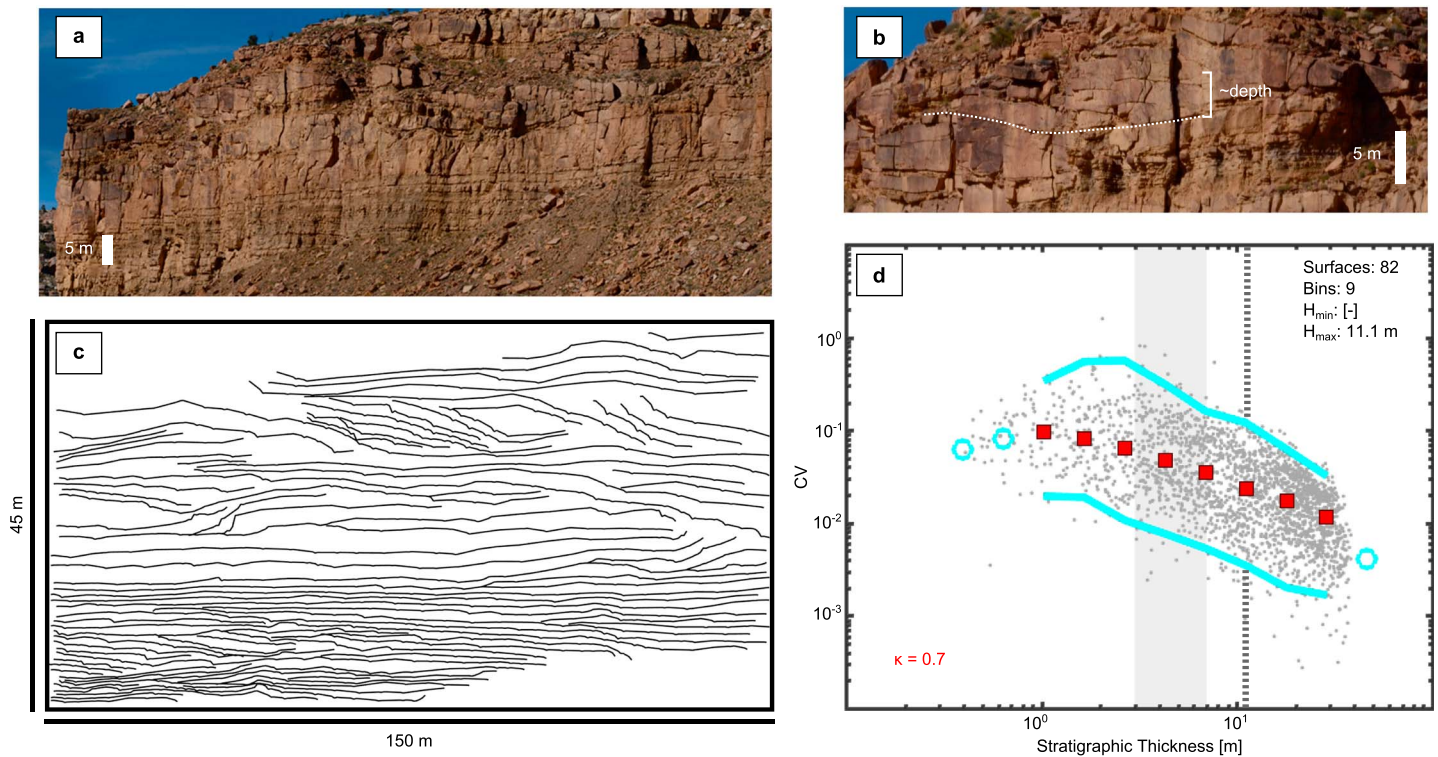
Figure 10. (a) Field photo of the Sego Sandstone outcrop in San Arroyo Canyon, Utah (supporting information). Mouth bar and channel sandstones are the cliff-forming layers. Paleoflow direction is into the cliff. (b) Field photograph of a representative channel sandstone in the Sego Sandstone. The height of the bar clinoforms dip down to the right (dashed white line) indicates a depth around 2 m. (c) Chronostratigraphic surfaces (271) for the Sego Sandstone. (d) Compensation statistic (*CV*) plot of the Sego Sandstone. The density of *CV* points is high over all and increases slightly at larger thicknesses. Bins below the mapping resolution (0.2 m) were excluded. The annotations are the same as in Figure 1.

4.2.2. Ferron Sandstone

The Ferron Sandstone (Turonian) is a member of the Mancos Shale and is interpreted as a river-dominated delta prograding northeastward into the Western Interior Seaway [*Cotter*, 1971; *Corbeanu et al.*, 2001; *Garrison and van den Bergh*, 2004; *Bhattacharya and MacEachern*, 2009; *Enge et al.*, 2010]. The studied outcrop of the upper Ferron Sandstone is located near Emery, Utah, in the "Last Chance Delta" portion of the Ferron Sandstone, specifically in parasequence set 2C of *Garrison and van den Bergh* [2004]. The outcrop consists primarily of mouth bar and distributary channel deposits; the outcrop was chosen to avoid major unconformities within the outcrop extent (Figure 11a). Channels from the Last Chance Delta are typically 3.9–5.2 m deep by 150–220 m wide [*Corbeanu et al.*, 2004]. We collected terrestrial lidar scans of the outcrop and mapped chronostratigraphic surfaces from digital outcrop models generated from the lidar scans. Additionally, we estimated channel depths and widths from clinoform geometries on the digital outcrop model; channel dimensions in the outcrop area are ~5 m deep and ~150 m wide (Figure 11b). Chronostratigraphic surfaces ($n = 82$) were mapped at bed-set boundary scale, with bed sets >40 cm resolved with confidence. Surfaces were projected onto a 2-D plane-parallel to the outcrop exposure, which is within 10° perpendicular to regional paleoflow direction (Figure 11c). Surfaces are discontinuous across the outcrop area. The outcrop is 9 times thicker than an individual channel element, although it is also only as wide as a single channel.

Compensation statistic values for the Ferron Sandstone were calculated over a range of 0.4–30 m. All *CV* points were aggregated into 11 logarithmic bins; the largest bin and smallest bins were excluded (Figure 11d). The density of *CV* points increases slightly over the entire range but is moderately low overall. We could not determine H_{min}; there are no scales that would result in a compensation index equal to 1.0. Additionally, scatter continues to decrease across the entire range, although the rate of reduction decreases near the bin centered at 11.1 m. The subcompensation index is 0.7, measured over the entire range of *CV* values.

The compensation scale of the Ferron Sandstone outcrop cannot be determined with confidence, but it is likely larger than the channel depth. The height of the Ferron Sandstone outcrop is about 7 times the local

Figure 11. (a) The upper Ferron Sandstone outcrop near Emery, Utah (supporting information). Mouth bar and channel sandstones are the cliff-forming layers. Flow is out of the cliff. (b) Field photograph of a representative channel sandstone in the Ferron Sandstone. The height of the bar clinoforms dip down to the right (dashed white line) indicates a paleoflow depth around 5 m. (c) Chronostratigraphic surfaces (82) for the Ferron Sandstone. Surfaces were mapped. (d) Compensation statistic (CV) plot of the Ferron Sandstone. H_{min} could not be determined. CV point density is low over all and does not greatly increase at larger thicknesses. There is a slight reduction of scatter at the bin centered at 11.1 m, but it is not pronounced. The annotations are the same as in Figure 1.

channel depth. Even with a very narrow outcrop the width of a single channel, a H_{min} smaller than 6 m should be detectable (e.g., Figure 4w). It is possible that a H_{min} between 6 and 15 m might be missed by the fitting procedure within some narrow outcrops (e.g., Figure 6b). There is a possible H_{max} at 11.1 m, but the reduction in scatter is not as clearly marked as in the experiment subsamples of a similar sized extent (Figure 6). We consider it likely that the compensation scale is larger than 12 m.

4.2.3. Comparison of Deltaic Case Studies

Unlike the fluvial case studies, both of the deltaic case studies were very small but relatively high resolution. The lower Sego Sandstone data set in particular is very high resolution, but the extent is very narrow. The autogenic sedimentation could reflect strong persistence due to the influence of tides within the Sego system or it could simply be a local aberration; to determine which of these interpretations is more likely, we would need data from more outcrops of similar size and quality from around the basin. The upper Ferron Sandstone shows signs of being extremely thin and narrow. Unlike the Sego data set, the Ferron Sandstone has a lower density of CV points, despite being mapped at a similar scale (i.e., bed-set resolution). This is likely because of how small the data set is both in width and thickness; the overall low density of CV values is most similar to the experiment subsamples that are less than three depositional elements thick and one depositional element wide. This would be consistent with a compensation scale that is much larger (i.e., over 10 m) than the observed channel depths. While the subcompensation index suggests that the Ferron data set demonstrates random sedimentation, it is impossible to determine what the autogenic sedimentation was without being able to determine H_{min} and without more data from around the basin.

Although both data sets are too small to be definitive, they suggest that there may be multiples scales of relief possible in deltaic deposits, similar to fluvial deposits. The compensation scale for the Sego Sandstone is consistent with the null hypothesis that channel depth is the main source of relief within deltaic systems [*Wang et al.*, 2011; *Straub and Wang*, 2013]. If the compensation scale of the Ferron Sandstone is

indeed larger than 10 m, this may indicate that basin depth, not channel depth, dominates compensation in some deltas. This is suggestive of the idea of foreset-dominated deltas and topset-dominated that has been proposed, where some deltas have thick foresets and thin topsets (foreset-dominated or "Gilbert-type" deltas) [*Edmonds et al.*, 2011b], but others have thick topsets and thin foresets (topset-dominated deltas) [*Edmonds et al.*, 2011b]. *Edmonds et al.* [2011b] predicts that in shallow, low-slope environments, the channel depth is able to incise deeper than the height of the foreset; in deep, high-slope environments, the foreset is much larger than the channel depth. It is possible that the Sego Sandstone developed in shallower water and is more consistent with a topset-dominated delta, whereas the Ferron Sandstone is more consistent with a deeper basin and is a foreset-dominated delta. However, the extents of both of our data sets are insufficient to fully investigate whether deltaic systems developed within deep and shallow basins have different compensation scales.

Both case studies provide an opportunity to explore the degree to which tides can alter the autogenic sedimentation patterns within deltaic deposits. The Sego Sandstone subcompensation index indicates strong persistence. Persistent behavior is consistent with the observed behavior of modern tide-dominated deltas, where tides have been observed to limit the mobility of distributary channels and also produce more regular bed-set thicknesses during the growth of tidal bars [e.g., *Dalrymple and Choi*, 2007; *Fagherazzi*, 2008; *Geleynse et al.*, 2011; *Leonardi et al.*, 2013]. Similarly, the Ferron Sandstone subcompensation index does suggest random to weakly compensational sedimentation. Random sedimentation is largely consistent with observations of a river-dominated delta, with presumably limited cohesion [*Edmonds and Slingerland*, 2007, 2010; *Nardin and Fagherazzi*, 2012; *Straub and Wang*, 2013; *Burpee et al.*, 2015]. However, we would need more data sets from both systems to determine whether these results truly reflect differences in the morphodynamics of each system, rather than being the result of local aberrations. Specifically, it would be necessary to have an extent wide enough to represent variability across the delta lobe, especially in the Ferron Sandstone which may be controlled by the lobe width and depth instead of the channel width and depth.

5. Discussion

Data set extent and resolution surprisingly do not seem to be major limitations of the compensation statistic, especially when using the compensation statistic to detect the compensation scale. As long as there are usable CV values below the zone of compensation, H_{min} and H_{max} can be reliably detected. Indeed, the most significant effect of resolution is on the low density of CV values below the zone of compensation which limits the use of the subcompensation index to describe autogenic sedimentation. For example, both fluvial case studies have very low density of CV values in their hypothesized compensation range; the density does not increase until after H_{max}. This is different than the overall low density of CV values that is common in very small data sets such as the Ferron data set, which has low density of points to either side of the hypothesized (channel depth) compensation range. Similarly, the extent needs to be at least 6 times the compensation scale to be sure to capture the compensation scale but is less sensitive to the lateral extent of the data set. Indeed, the primary effect of narrow extents is that the subcompensation index tends to reflect local autogenic behaviors instead of the system-wide average, which may be an advantage in some situations.

While we focused on cross sections that are perpendicular to paleoflow for our analyses, the compensation statistic can still be applied to cross sections of different orientations. When the compensation statistic is applied to oblique cross sections, the extent should be scaled to the apparent thickness and width of the depositional unit (e.g., channel, lobe, or sand body scale). Unless there is a systematic change in the paleoflow direction across the data set, the compensation statistic should be comparable between cross sections with different orientations. However, oblique sections in heavily channelized deposits are likely to underestimate the compensation scale and the subcompensation index (i.e., the subcompensation index will look more persistent), since the probability of seeing the maximum amount of variability is reduced in oblique cuts (e.g., channel scour or levee deposition is more likely to be measurable in a section that is approximately perpendicular to the paleoflow direction). A system where the depositional element is more lobe-like would likely be less sensitive to the orientation of the cross section.

The maximum autogenic scale is a consequence of the distribution of depositional and erosional scales possible within a depositional environment. The maximum relief that a system can produce depends heavily on the specific morphodynamics of the individual depositional system. The simplest source of relief that all fluvial and deltaic systems share is channel scour, but larger sources of relief (e.g., alluvial ridge, megafan, and

delta foreset) may or may not exist in any given system. If the compensation statistic is to be useful for hypothesis testing, it must be able to distinguish between these different scales of relief.

Both the fluvial and deltaic case studies demonstrate the utility of the compensation scale to test hypotheses about the largest scale of relief that can be developed within a system. Within fluvial environments, there has been a question whether the largest autogenic landform equates primarily to a channel scour, an entire channel-belt-scale alluvial ridge, or some larger megafan feature [*Mohrig et al.*, 2000; *Hartley et al.*, 2010; *Hajek and Heller*, 2012; *Hajek and Wolinsky*, 2012; *Edmonds et al.*, 2016]. Both the Ferris Formation and lower Williams Fork Formation data sets have compensation scales much larger than the size of their channel scours, although rivers in the Ferris Formation may have been able to produce much more relief relative to their channel depth than the lower Williams Fork Formation. This underscores the potential importance of long-term sediment storage-and-release episodes in some fluvial landscapes [e.g., *Dalman and Weltje*, 2008; *Kim and Jerolmack*, 2008].

Similarly, there is a question about if and when the autogenic dynamics of deltaic systems should be controlled by the delta's fluvial topset (H_{max}~channel depth) or the relief of the delta foreset (H_{max}~basin depth) [e.g., *Muto and Steel*, 2004; *Muto et al.*, 2007; *Kim and Jerolmack*, 2008]. Basin depth and subsidence patterns influence how sediment is partitioned between the fluvial topset and the subaqueous foreset during delta growth [*Cederberg*, 2014; *Hajek et al.*, 2014; *Leva Lopez et al.*, 2014]. When delta mass is sequestered in the fluvial topset, fluvial-system scale may be the dominant influence on autogenic dynamics; however, in systems where the balance of sediment is in the delta foreset, basin depth and growth may set autogenic sedimentation patterns. In our deltaic case studies, the lower Sego Sandstone has a compensation scale consistent with channel depth, but the upper Ferron Sandstone has a compensation depth that is at least 2 or 3 times larger. It is possible that Ferron compensation scale is more reflective of basin depth (where the delta front clinoform would be the largest source of "relief" in the system) rather than morphodynamic organization of the delta topset.

The subcompensation index can also be a valuable hypothesis-testing tool to describe characteristic autogenic sedimentation patterns, especially when used in conjunction with other statistical analyses. With extensive, well-resolved data sets, subcompensation index values are describing average autogenic sedimentation patterns and can be used to readily distinguish persistent (or clustered) sedimentation from compensational sedimentation. However, a random value (e.g., ~$0.4 < \kappa < $~$0.6$) may indicate either truly random sedimentation or a mixture of persistent and compensational sedimentation.

Another consideration is the degree to which an individual subcompensation index value reflects local sediment dynamics versus system-wide autogenic behavior. In general, the smaller data sets should reflect more local conditions. However, assemblages of small data sets can give insight into the larger-scale, system-wide landscape dynamics. For example, Figures 5 and 6 demonstrate that while the entire experiment has a subcompensation index that indicates random sedimentation, the subcompensation indices of small subsamples span the range of random, persistent, and compensational sedimentation. This suggests that the experiment TDB 10-1 may be (weakly) clustered instead of purely randomly organized. We suggest that in systems where large data set extents are not possible, the assemblages of small data sets may be used to infer system-wide autogenic organization.

6. Conclusions

1. We can reliably estimate the maximum autogenic scale using the compensation statistic. The compensation statistic is relatively insensitive to the extent and resolution typical in outcrop data. We have shown that some fluvial and deltaic systems, such as the Ferris Formation and the lower Williams Fork Formation, have a maximum autogenic scale much larger than what would be predicted based on the channel geometry.
2. We can use the compensation statistic to gain valuable insight into autogenic (subcompensation) sedimentation within ancient fluvial and deltaic systems, especially when it is used in combination with other metrics and observations. The subcompensation index reflects system morphodynamics, although it is much more sensitive to data-handling choices than the compensation scale. We have shown that there is persistent sedimentation in the tide-dominated Sego Sandstone but random to weakly compensational organization within the river-dominated Ferron Sandstone.

3. We recommend that the compensation statistic is best applied to data sets that are thicker than 6 times the anticipated compensation scale and with a resolution sufficiently smaller than the anticipated compensation scale to ensure that the compensation scale can be identified. Narrow lateral extents demonstrate variable, local autogenic behavior, whereas wider extents can be used to determine system-wide, average autogenic behavior.

4. Our analyses provide guidelines for constraining the scale of effective morphodynamics in ancient systems. Both compensation scale (i.e., maximum autogenic scale) and subcompensation organization (i.e., patterns of autogenic sedimentation) can be investigated in data sets with a wide range of data extents and resolutions. The robustness of the compensation statistic opens up a rich range of questions about allogenic and autogenic processes that operate at long time scales within many fluvial and deltaic deposits.

References

Ashton, A. D., and L. Giosan (2011), Wave-angle control of delta evolution, *Geophys. Res. Lett.*, 38, L13405, doi:10.1029/2011GL047630.

Bhattacharya, J. P., and J. A. MacEachern (2009), Hyperpycnal rivers and prodeltaic shelves in the cretaceous seaway of North America, *J. Sediment. Res.*, 79, 184–209, doi:10.2110/jsr.2009.026.

Bhattacharya, J. P., and L. Giosan (2003), Wave-influenced deltas: Geomorphological implications for facies reconstruction, *Sedimentology*, 50, 187–210, doi:10.1046/j.1365-3091.2003.00545.x.

Bhattacharyya, P., J. P. Bhattacharya, and S. D. Khan (2015), Paleo-channel reconstruction and grain size variability in fluvial deposits, Ferron Sandstone, Notom Delta, Hanksville, Utah, *Sediment. Geol.*, 325, 17–25, doi:10.1016/j.sedgeo.2015.05.001.

Burpee, A. P., R. L. Slingerland, D. A. Edmonds, D. Parsons, J. Best, J. A. Cederberg, A. McGuffin, R. Caldwell, A. Nijhuis, and J. Royce (2015), Grain-size controls on the morphology and internal geometry of river-dominated deltas, *J. Sediment. Res.*, 85(6), 699–714, doi:10.2110/jsr.2015.39.

Cederberg, J. A. (2014), A quantitative assessment of the effects of base level fall and basin depth on river-dominated deltas MS thesis, The Pennsylvania State Univ.

Chamberlin, E. P., and E. A. Hajek (2015), Interpreting paleo-avulsion dynamics from multistory sand bodies, *J. Sediment. Res.*, 85(2), 82–94, doi:10.2110/jsr.2015.09.

Chamberlin, E. P., E. A. Hajek, and S. M. Trampush (2016), Measuring scales of autogenic organization in fluvial stratigraphy: An example from the Cretaceous lower Williams Fork Formation, Colorado, USA, *Autogenic Dyn. Self-Organ. Sediment. Syst.*, 106, doi:10.2110/sepmsp.106.07.

Clauset, A., C. R. Shalizi, and M. E. J. Newman (2009), Power-law distributions in empirical data, *SIAM Rev.*, 51(4), 661–703, doi:10.1137/070710111.

Cole, R., and S. P. Cumella (2005), Sand-body architecture in the lower Williams Fork Formation (Upper Cretaceous), Coal Canyon, Colorado, with comparison to the Piceance Basin subsurface, *Mt. Geol.*, 42(3), 85–107.

Corbeanu, R. M., K. Soegaard, R. B. Szerbiak, J. B. Thurmond, G. A. McMechan, D. Wang, S. Snelgrove, C. B. Forster, and A. Menitove (2001), Detailed internal architecture of a fluvial channel sandstone determined from outcrop, cores, and 3-D ground-penetrating radar: Example from the middle Cretaceous Ferron Sandstone, east-central Utah, *Am. Assoc. Pet. Geol. Bull.*, 85(9), 1583–1608, doi:10.1306/8626CCCB-173B-11D7-8645000102C1865D.

Corbeanu, R. M., M. C. Wizevich, J. P. Bhattacharya, X. Zeng, and G. A. McMechan (2004), Three-dimensional architecture of ancient lower delta-plain point bars using ground-penetrating radar, Cretaceous Ferron Sandstone, Utah, *AAPG Stud. Geol.*, 50, 427–449.

Cotter, E. (1971), Paleoflow characteristics of a Late Cretaceous river in Utah from analysis of sedimentary structures in the Ferron Sandstone, *J. Sediment. Res.*, 41, 129–138, doi:10.1306/74D72202-2B21-11D7-8648000102C1865D.

Dalman, R. A. F., and G. J. Weltje (2008), Sub-grid parameterisation of fluvio-deltaic processes and architecture in a basin-scale stratigraphic model, *Comput. Geosci.*, 34(10), 1370–1380, doi:10.1016/j.cageo.2008.02.005.

Dalrymple, R. W., and K. Choi (2007), Morphologic and facies trends through the fluvial-marine transition in tide-dominated depositional systems: A schematic framework for environmental and sequence-stratigraphic interpretation, *Earth-Science Rev.*, 81, 135–174, doi:10.1016/j.earscirev.2006.10.002.

Edmonds, D. A., and R. L. Slingerland (2007), Mechanics of river mouth bar formation: Implications for the morphodynamics of delta distributary networks, *J. Geophys. Res.*, 112, F02034, doi:10.1029/2006JF000574.

Edmonds, D. A., and R. L. Slingerland (2010), Significant effect of sediment cohesion on delta morphology, *Nat. Geosci.*, 3(2), 105–109, doi:10.1038/ngeo730.

Edmonds, D. A., C. Paola, D. Hoyal, and B. A. Sheets (2011a), Quantitative metrics that describe river deltas and their channel networks, *J. Geophys. Res.*, 116, F04022, doi:10.1029/2010JF001955.

Edmonds, D. A., J. B. Shaw, and D. Mohrig (2011b), Topset-dominated deltas: A new model for river delta stratigraphy, *Geology*, 39(12), 1175–1178, doi:10.1130/G32358.1.

Edmonds, D. A., E. A. Hajek, N. Downton, and A. B. Bryk (2016), Avulsion flow-path selection on rivers in foreland basins, *Geology*, 44(9), G38082.1, doi:10.1130/G38082.1.

Enge, H. D., J. A. Howell, and S. J. Buckley (2010), The geometry and internal architecture of stream mouth bars in the Panther Tongue and the Ferron Sandstone Members, Utah, U.S.A, *J. Sediment. Res.*, 80, 1018–1031, doi:10.2110/jsr.2010.088.

Fagherazzi, S. (2008), Self-organization of tidal deltas, *Proc. Natl. Acad. Sci. U.S.A.*, 105, 18,692–18,695, doi:10.1073/pnas.0806668105.

Farrell, K. M. (2001), Geomorphology, facies architecture, and high-resolution, non-marine sequence stratigraphy in avulsion deposits, Cumberland Marshes, Saskatchewan, *Sediment. Geol.*, 139, 93–150, doi:10.1016/S0037-0738(00)00150-0.

Fielding, C. R. (2010), Planform and facies variability in asymmetric deltas: Facies analysis and depositional architecture of the Turonian Ferron Sandstone in the Western Henry Mountains, south-central Utah, U.S.A, *J. Sediment. Res.*, 80, 455–479, doi:10.2110/jsr.2010.047.

Flood, Y. S., and G. J. Hampson (2015), Quantitative analysis of the dimensions and distribution of channelized fluvial sand bodies within a large outcrop dataset: Upper Cretaceous Blackhawk Formation, Wasatch Plateau, central Utah, U.S.A, *J. Sediment. Res.*, 85, 315–336, doi:10.2110/jsr.2015.25.

Ganti, V., M. P. Lamb, and B. McElroy (2014), Quantitative bounds on morphodynamics and implications for reading the sedimentary record, *Nat. Commun.*, 5, 3298, doi:10.1038/ncomms4298.

Garrison, J. R. J., and T. C. V. van den Bergh (2004), High-resolution depositional sequence stratigraphy of the Upper Ferron Sandstone Last Chance Delta: An application of coal-zone stratigraphy, *AAPG Stud. Geol.*, *50*, 125–192.

Geleynse, N., J. E. A. Storms, D. J. R. Walstra, H. R. A. Jagers, Z. B. Wang, and M. J. F. Stive (2011), Controls on river delta formation; insights from numerical modelling, *Earth Planet. Sci. Lett.*, *302*(1–2), 217–226, doi:10.1016/j.epsl.2010.12.013.

Hajek, E. A., and M. A. Wolinsky (2012), Simplified process modeling of river avulsion and alluvial architecture: Connecting models and field data, *Sediment. Geol.*, *257–260*, 1–30, doi:10.1016/j.sedgeo.2011.09.005.

Hajek, E. A., and P. L. Heller (2012), Flow-depth scaling in alluvial architecture and nonmarine sequence stratigraphy: Example from the Castlegate Sandstone, central Utah, U.S.A, *J. Sediment. Res.*, *82*, 121–130, doi:10.2110/jsr.2012.8.

Hajek, E. A., P. L. Heller, and B. A. Sheets (2010), Significance of channel-belt clustering in alluvial basins, *Geology*, *38*, 535–538, doi:10.1130/G30783.1.

Hajek, E. A., P. L. Heller, and E. L. Schur (2012), Field test of autogenic control on alluvial stratigraphy (Ferris Formation, Upper Cretaceous-Paleogene, Wyoming), *GSA Bull.*, *124*(11), 1898–1912, doi:10.1130/B30526.1.

Hajek, E., C. Paola, A. Petter, A. Alabbad, and W. Kim (2014), Amplification of shoreline response to sea-level change by back-tilted subsidence, *J. Sediment. Res.*, *84*(6), 470–474, doi:10.2110/jsr.2014.34.

Hartley, A. J., G. S. Weissmann, G. J. Nichols, and L. A. Scuderi (2010), Fluvial form in modern continental sedimentary basins: Distributive fluvial systems: REPLY, *Geology*, *38*(12), e231, doi:10.1130/G31588Y.1.

Hofmann, M. H., A. Wroblewski, and R. Boyd (2011), Mechanisms controlling the clustering of fluvial channels and the compensational stacking of cluster belts, *J. Sediment. Res.*, *81*, 670–685, doi:10.2110/jsr.2011.54.

Hoyal, D. C. J. D., and B. A. Sheets (2009), Morphodynamic evolution of experimental cohesive deltas, *J. Geophys. Res.*, *114*, F02009, doi:10.1029/2007JF000882.

Jerolmack, D. J., and C. Paola (2010), Shredding of environmental signals by sediment transport, *Geophys. Res. Lett.*, *37*, 1–6, doi:10.1029/2010GL044638.

Jerolmack, D. J., and J. B. Swenson (2007), Scaling relationships and evolution of distributary networks on wave-influenced deltas, *Geophys. Res. Lett.*, *34*, L23402, doi:10.1029/2007GL031823.

Jones, C. R., J. C. Van Wagoner, T. M. Demko, R. W. Wellner, G. G. Mccrimmon, S. T. Hasiotis, R. T. Beaubouef, and H. R. Feldman (2002), Large, prograding fluvial megafan complexes: Influence of climate cyclicity on reservoir architecture Am. Assoc. of Pet. Geol. Annual Meeting, p. 90007, Houston, Tex.

Kim, W., and D. J. Jerolmack (2008), The pulse of calm fan deltas, *J. Geol.*, *116*, 315–330, doi:10.1086/588830.

Leier, A. L., P. G. DeCelles, and J. D. Pelletier (2005), Mountains, monsoons, and megafans, *Geology*, *33*(4), 289–292, doi:10.1130/G21228.1.

Leonardi, N., A. Canestrelli, T. Sun, and S. Fagherazzi (2013), Effect of tides on mouth bar morphology and hydrodynamics, *J. Geophys. Res. Ocean.*, *118*, 4169–4183, doi:10.1002/jgrc.20302.

Leva Lopez, J., W. Kim, and R. J. Steel (2014), Autoacceleration of clinoform progradation in foreland basins: Theory and experiments, *Basin Res.*, *26*(4), 489–504, doi:10.1111/bre.12048.

Li, Q., L. Lu, and K. M. Straub (2016), Storage thresholds for relative sea-level signals in the stratigraphic record, *Geology*, *44*(3), 179–182, doi:10.1130/G37484.1.

Lillegraven, J. A., A. W. Snoke, and M. C. McKenna (2004), Tectonic and paleogeographic implications of late Laramide geologic history in the northeastern corner of Wyoming's Hanna Basin, *Rocky Mt. Geol.*, *39*(1), 7–64.

Lyons, W. J. (2004), Quantifying channelized submarine depositional systems from bed to basin scale PhD dissertation, Massachusetts Institute of Technology, Cambridge.

Martin, J., B. Sheets, C. Paola, and D. Hoyal (2009), Influence of steady base-level rise on channel mobility, shoreline migration, and scaling properties of a cohesive experimental delta, *J. Geophys. Res.*, *114*, F03017, doi:10.1029/2008JF001142.

Mohrig, D., P. L. Heller, C. Paola, and W. J. Lyons (2000), Interpreting avulsion process from ancient alluvial sequences: Guadalope-Matarranya system (northern Spain) and Wasatch Formation (western Colorado), *GSA Bull.*, *112*, 1787–1803, doi:10.1130/0016-7606(2000)112<1787:IAPFAA>2.0.CO;2.

Muto, T., and R. J. Steel (2004), Autogenic response of fluvial deltas to steady sea-level fall: Implications from flume-tank experiments, *Geology*, *32*(5), 401–404, doi:10.1130/G20269.1.

Muto, T., R. J. Steel, and J. B. Swenson (2007), Autostratigraphy: A framework norm for genetic stratigraphy, *J. Sediment. Res.*, *77*(1), 2–12, doi:10.2110/jsr.2007.005.

Nardin, W., and S. Fagherazzi (2012), The effect of wind waves on the development of river mouth bars, *Geophys. Res. Lett.*, *39*, L12607, doi:10.1029/2012GL051788.

Newman, M. E. J. (2005), Power laws, Pareto distributions and Zipf's law, *Contemp. Phys.*, *46*(5), 323–351, doi:10.1016/j.cities.2012.03.001.

Nienhuis, J. H., A. D. Ashton, P. C. Roos, S. J. M. H. Hulscher, and L. Giosan (2013), Wave reworking of abandoned deltas, *Geophys. Res. Lett.*, *40*, 5899–5903, doi:10.1002/2013GL058231.

Olariu, C., and J. P. Bhattacharya (2006), Terminal distributary channels and delta front architecture of river-dominated delta systems, *J. Sediment. Res.*, *76*, 212–233, doi:10.2110/jsr.2006.026.

Olariu, M. I., C. Olariu, R. J. Steel, R. W. Dalrymple, and A. W. Martinius (2012), Anatomy of a laterally migrating tidal bar in front of a delta system: Esdolomada Member, Roda Formation, Tremp-Graus Basin, Spain, *Sedimentology*, *59*, 356–378, doi:10.1111/j.1365-3091.2011.01253.x.

Pederson, C. A., P. M. Santi, and D. R. Pyles (2015), Relating the compensational stacking of debris-flow fans to characteristics of their underlying stratigraphy: Implications for geologic hazard assessment and mitigation, *Geomorphology*, *248*, 47–56, doi:10.1016/j.geomorph.2015.06.030.

Pranter, M. J., R. D. Cole, H. Panjaitan, and N. K. Sommer (2009), Sandstone-body dimensions in a lower coastal-plain depositional setting: Lower Williams Fork Formation, Coal Canyon, Piceance Basin, Colorado, *Am. Assoc. Pet. Geol. Bull.*, *93*(10), 1379–1401, doi:10.1306/06240908173.

Schomacker, E. R., A. V. Kjemperud, J. P. Nystuen, and J. S. Jahren (2010), Recognition and significance of sharp-based mouth-bar deposits in the Eocene Green River Formation, Uinta Basin, Utah, *Sedimentology*, *57*(4), 1069–1087, doi:10.1111/j.1365-3091.2009.01136.x.

Sheets, B. A., T. A. Hickson, and C. Paola (2002), Assembling the stratigraphic record: Depositional patterns and time-scales in an experimental alluvial basin, *Basin Res.*, *14*, 287–301.

Straub, K. M., and C. R. Esposito (2013), Influence of water and sediment supply on the stratigraphic record of alluvial fans and deltas: Process controls on stratigraphic completeness, *J. Geophys. Res. Earth Surf.*, *118*, 625–637, doi:10.1002/jgrf.20061.

Straub, K. M., and D. R. Pyles (2012), Quantifying the hierarchical organization of compensation in submarine fans using surface statistics, *J. Sediment. Res.*, *82*(1981), 889–898, doi:10.2110/jsr.2012.73.

Straub, K. M., and Y. Wang (2013), Influence of water and sediment supply on the long-term evolution of alluvial fans and deltas: Statistical characterization of basin-filling sedimentation patterns, *J. Geophys. Res. Earth Surf.*, *118*, 1602–1616, doi:10.1002/jgrf.20095.

Straub, K. M., C. Paola, D. Mohrig, M. A. Wolinsky, and T. George (2009), Compensational stacking of channelized sedimentary deposits, *J. Sediment. Res.*, *79*(1981), 673–688, doi:10.2110/jsr.2009.070.

Tornqvist, T. E., and J. S. Bridge (2002), Spatial variation of overbank aggradation rate and its influence on avulsion frequency, *Sedimentology*, *49*, 891–905, doi:10.1046/j.1365-3091.2002.00478.x.

Van Wagoner, J. C., and R. M. Mitchum (1990), Siliciclastic sequence stratigraphy in well logs, cores, and outcrops: Concepts for high-resolution correlation of time and facies, in *Siliciclastic Seq. Stratigr. Well Logs, Cores, Outcrops Concepts High-Resolution Correl. Time Facies*, *Methods Explor. Ser.*, vol. 7, pp. 3–55 , Am. Assoc. of Pet. Geol., Tulsa, Okla.

Wang, Y., K. M. Straub, and E. A. Hajek (2011), Scale-dependent compensational stacking: An estimate of autogenic time scales in channelized sedimentary deposits, *Geology*, *39*(9), 811–814, doi:10.1130/G32068.1.

Weimer, R. J. (1984), Relation of unconformities, tectonics, and sea-level changes, Cretaceous of Western Interior, U.S.A., in *Interregional Unconformities and Hydrocarbon Accumulation*, *Mem.*, vol. 36, edited by J. S. Schlee, pp. 7–35 , Am. Assoc. of Pet. Geol., Tulsa, Okla.

Weissmann, G. S., A. J. Hartley, G. J. Nichols, L. A. Scuderi, M. Olson, H. Buehler, and R. Banteah (2010), Fluvial form in modern continental sedimentary basins: Distributive fluvial systems, *Geology*, *38*(1), 39–42, doi:10.1130/G30242.1.

Willis, A. (2000), Tectonic control of nested sequence architecture in the Sego Sandstone, Neslen Formation and Upper Castlegate Sandstone (Upper Cretaceous), Sevier Foreland Basin, Utah, USA, *Sediment. Geol.*, *136*, 277–317, doi:10.1016/S0037-0738(00)00087-7.

Willis, B. J., and S. Gabel (2001), Sharp-based, tide-dominated deltas of the Sego Sandstone, Book Cliffs, Utah, USA, *Sedimentology*, *48*, 479–506, doi:10.1046/j.1365-3091.2001.00363.x.

Willis, B. J., and S. L. Gabel (2003), Formation of deep incisions into tide-dominated river deltas: Implications for the stratigraphy of the Sego Sandstone, Book Cliffs, Utah, U.S.A, *J. Sediment. Res.*, *73*(1996), 246–263, doi:10.1306/090602730246.